Accepted for publication in ***Building & Environment****, 4 February 2016*

Review and position paper

Pedestrian-level wind conditions around buildings: review of wind-tunnel and CFD techniques and their accuracy for wind comfort assessment

B. Blocken [(a,b)]*, T. Stathopoulos [(c)], J.P.A.J. van Beeck [(d)]

(a) Building Physics and Services, Department of the Built Environment, Eindhoven University of Technology, P.O. box 513, 5600 MB Eindhoven, The Netherlands

(b) Building Physics Section, Department of Civil Engineering, KU Leuven, Kasteelpark Arenberg 40 – bus 2447, 3001 Leuven, Belgium

(c) Centre for Building Studies, Department of Building, Civil and Environmental Engineering, Concordia University, 1455 de Maisonneuve Blvd. West, Montreal, Quebec, Canada H3G1M8

(d) Environmental & Applied Fluid Dynamics Department, von Karman Institute for Fluid Dynamics, 1640 Sint-Genesius-Rode, Belgium

Abstract

Information on pedestrian-level wind (PLW) speed for wind comfort assessment can be obtained by wind-tunnel measurements or Computational Fluid Dynamics (CFD) simulations. Wind-tunnel measurements for PLW are routinely performed with low-cost techniques such as hot-wire or hot-film anemometers, Irwin probes or sand erosion, while Laser-Doppler Anemometry (LDA) and Particle-Image Velocimetry (PIV) are less often used because they are more expensive. CFD simulations are routinely performed by the relatively low-cost steady Reynolds-Averaged Navier-Stokes (RANS) approach. Large-Eddy Simulation (LES) is less often used because of its larger complexity and cost. This paper reviews wind-tunnel and CFD techniques to determine PLW speeds expressed generally in terms of amplification factors defined as the ratio of local mean wind speed to mean wind speed at the same position without buildings present. Some comparative studies systematically indicate that the low-cost wind-tunnel techniques and steady RANS simulations can provide accurate results (~10%) at high amplification factors (> 1) while their accuracy can deteriorate at lower amplification factors (< 1). This does not necessarily compromise the accuracy of PLW comfort assessment, because the higher amplification factors provide the largest contribution to the discomfort exceedance probability in the comfort criterion. Although LDA, PIV and LES are inherently more accurate techniques, this paper supports the continued use of faster and more inexpensive techniques for PLW studies. Extrapolating a previous saying, we argue that pedestrian-level wind comfort is one of the few topics in wind engineering where nature is kind to us concerning turbulent flows.

Keywords: Overview; wind environment; CFD simulation; urban area; building aerodynamics; urban physics.

List of acronyms

ABL	Atmospheric boundary layer
AIAA	American Institute of Aeronautics and Astronautics
AIJ	Architectural Institute of Japan
ASCE	American Society of Civil Engineers
ASME	Americal Society of Mechanical Engineers
BFS	Backward facing step
BLWTL	Boundary layer wind tunnel laboratory
CCA	Constant-current anemometry
CFD	Computational Fluid Dynamics
COST	European Cooperation in Science and Technology
CTA	Constant-temperature anemometry

* **Corresponding author**: Bert Blocken, Building Physics and Services, Eindhoven University of Technology, P.O.Box 513, 5600 MB Eindhoven, the Netherlands. Tel.: +31 (0)40 247 2138, Fax +31 (0)40 243 8595
E-mail address: b.j.e.blocken@tue.nl

CVA	Constant-voltage anemometry
CWE	Computational wind engineering
ECORA	Evaluation of Computational Fluid Dynamic Methods for Reactor Safety Analysis
ERCOFTAC	European Research Community on Flow, Turbulence and Combustion
HFA	Hot-film anemometry
HWA	Hot-wire anemometry
LDA	Laser-doppler anemometry
LDV	Laser-doppler velocimetry
LES	Large-eddy simulation
NEN	Nederlandse norm (Dutch Standard)
NS	Navier-Stokes
PIV	Particle-image velocimetry
PLW	Pedestrian-level wind
PWA	Pulsed-wire anemometry
QNET –CFD	Network for Quality and Trust in the Industrial Application of CFD
RANS	Reynolds-averaged Navier-Stokes
RMS	Root mean square
RNG	Renormalization group
RSM	Reynolds stress model
SST	Shear-stress transport
SWS	Surface wind sensor
URANS	Unsteady Reynolds-Averaged Navier-Stokes
VKI	Von Karman Institute for Fluid Dynamics

1. Introduction

High-rise buildings can introduce high wind speed at pedestrian level, which can lead to uncomfortable or even dangerous conditions. Wind discomfort can be detrimental to the success of new buildings. In 1970, Wise [1] reported about shops that are left untenanted because of the windy environment which discouraged shoppers. Lawson and Penwarden [2] reported the death of two old ladies due to an unfortunate fall caused by high wind speed at the base of a tall building. Nowadays, many urban authorities only grant a building permit for a new high-rise building after a wind comfort study has indicated that the negative consequences for the pedestrian wind environment remain limited. Although thermal comfort is also important (e.g. [3-7]) and humidity, solar radiation and precipitation also play an important role [4,5,8-10], wind comfort generally only refers to the mechanical effects of wind on people (e.g. [2,11]).

A PLW comfort study should be performed by a combination of three types of information/data: (1) statistical meteorological data; (2) aerodynamic information; and (3) a comfort criterion. The aerodynamic information is needed to transform the statistical meteorological data from the weather station (meteorological site) to the location of interest at the building site. At this location, the transformed statistical data are combined with the comfort criterion to assess local wind comfort. This procedure is schematically depicted in Figure 1. Wind statistics at the meteorological site can be expressed as potential wind speed (U_{pot}), i.e. corresponding to a terrain with aerodynamic roughness length $z_0 = 0.03$ m [12]. The aerodynamic information usually consists of two parts: the terrain-related contribution and the design-related contribution. The terrain-related contribution represents the change in wind statistics from the meteorological site to a reference location near or at the building site, i.e. the transformation of U_{pot} to U_0. The design-related contribution represents the change in wind statistics due to the local urban design, i.e. the transformation of U_0 to the local wind speed U. Information on transformation procedures to determine terrain-related contributions can be found in e.g. [13-15]. The design-related contribution (i.e. the wind flow conditions around the buildings at the building site) is generally obtained by either wind-tunnel testing or numerical simulation with Computational Fluid Dynamics (CFD).

Wind comfort criteria generally exist of a threshold value U_{THR} for the effective wind speed U_e and a maximum allowed exceedance probability P of this threshold. The effective wind speed is defined as:

$$U_e = U + k\sigma_u$$

where U is the mean wind speed, k the peak factor (generally between 0 and 3.5) and σ_u the root mean square (rms) wind speed. Reviews on comfort criteria have been provided by Bottema [16], Koss [17] and Janssen et al. [18]. As an example, Table 1 shows the comfort criterion and Table 2 the safety criterion in the Dutch Wind

Nuisance Standard NEN 8100 [19], which is – to the best of our knowledge – the first and to the present day the only wind comfort standard in the world. In this standard the threshold wind speed for wind comfort is 5 m/s, the peak factor k is 0 and different exceedance probabilities point to different comfort classes for three types of activities: traversing, strolling and sitting. An overview of some other wind comfort criteria and their comparison with the NEN 8100 criterion is given in Table 3.

As mentioned earlier, the design-related contribution is generally obtained by either wind-tunnel testing or numerical simulation with CFD. Wind-tunnel measurements for PLW can be performed with low-cost techniques such as hot-wire or hot-film anemometry (HWA or HFA) (e.g. [23-33], pulsed-wire anemometry (PWA) (e.g. [34-36]), Irwin probes (e.g. [37-42]) or sand erosion (e.g. [30,38,.41,43-49]). On a few occasions, also infrared thermography has been used (e.g. [50-52]). Laser-Doppler Anemometry (LDA) (e.g. [41]) and Particle Image Velocimetry (PIV) (e.g. [41]) are less often used because they are more elaborate and more expensive.

CFD simulations of PLW are routinely performed by the relatively low-cost 3D steady Reynolds-Averaged Navier-Stokes (RANS) approach (e.g. [21,33,48,53-85]), while Large Eddy Simulation (LES) is less often used because of its larger complexity and computational cost. Some exceptions of PLW studies with LES are the studies by He and Song [86] and Razak et al. [87].

The question arises whether "less accurate" but less expensive and faster techniques such as HWA, HFA, Irwin probes, sand erosion and 3D steady RANS CFD simulations can provide sufficiently accurate data on mean wind speed for PLW comfort assessment. If so, this would justify the vast majority of past research efforts and support the continued use of these low-cost and relatively fast techniques for this type of studies. If not, this would motivate the transition to more expensive techniques such as LDA, PIV and LES. This paper attempts to answer this question.

This paper is a combination of a review and a position paper. In the past, several review and overview papers addressing PLW or even exclusively focused on PLW have been published. Wind-tunnel techniques were reviewed by Ettouney and Fricke [88], Irwin [89], Beranek [90], Wu and Stathopoulos [91] and ASCE [4,5]. Wind-tunnel and/or CFD techniques applied to PLW were reviewed by Stathopoulos [6,92,93], Blocken et al. [70,94], Moonen et al. [79], Blocken and Stathopoulos [95] and Blocken [82,83]. PLW was also addressed in several reports and books [4,5,96,97]. The present paper differs from these previous review documents because of four reasons: (1) It focuses on a wider range of wind-tunnel techniques; (2) It focuses on comparisons between different wind-tunnel techniques to assess their accuracy; (3) It addresses both wind-tunnel and CFD techniques, including comparisons between both; (4) It focuses on the accuracy of wind comfort and wind danger assessment by analyzing how errors in the prediction of mean wind speed – by either wind-tunnel or CFD techniques – propagate to the overall assessment of wind comfort.

The paper is structured as follows: In section 2, a review of wind-tunnel techniques for PLW is provided. Section 3 reviews studies on the accuracy of these wind-tunnel techniques for PLW. In section 4, some best practice guidelines for wind-tunnel testing of PLW are outlined. Section 5 contains a review of CFD techniques for PLW. Section 6 reviews studies on the accuracy of CFD techniques for PLW. In section 7, best practice guidelines for CFD simulation of PLW are presented. Section 8 consists of a simple wind comfort assessment study to demonstrate to what extent wind-tunnel or CFD errors in mean wind speed propagate to the overall wind comfort assessment. Sections 9 (discussion) and 10 (conclusions) complete the paper.

2. Wind-tunnel techniques for pedestrian-level wind speed measurements

Hot-wire anemometry (HWA), hot-film anemometry (HFA), pulsed-wire anemometry (PWA) and laser-Doppler anemometry (LDA) are classified as "point measurement" techniques, although strictly they measure the air speed over a small area or volume. Irwin sensors also provide point measurements, while scour techniques (such as sand erosion), infrared thermography and Particle Image Velocimetry (PIV) are area techniques that provide spatially continuous information on the flow conditions over a large part (or the whole) of the area under study.

2.1. Hot-wire anemometry

Only single-wire measurements as commonly used in PLW studies are addressed. HWA uses a very fine wire (1 to 10 μm diameter) with a length of 0.5 to 3 mm with a high temperature coefficient of resistance such as tungsten, platinum, platinum-rhodium, and platinum-iridium (Fig. 2a). For PLW studies, the single wire should be positioned vertically in the wind tunnel, to measure the horizontal wind components and provide an average speed over the wire length. The wire is electrically heated up to a temperature substantially above the ambient temperature (typically 180 to 200 K temperature difference in gases) and the flow past the wire exerts a cooling effect on it. A distinction is made between CCA (constant-current anemometry), CVA (constant-voltage anemometry) and CTA (constant-temperature anemometry). The voltage output from these anemometers results from trying to maintain the specific variable (current, voltage or temperature) constant according to Ohm's law.

The relationship between the resistance of the wire and the flow speed is then used to obtain an estimate of this flow speed.

Advantages of HWA are the very high frequency-response (up to 10 kHz) and the high spatial resolution due to the small dimensions. HWA has been used extensively in PLW studies. Durgin [38] labels it even as "ideal for measuring PLWs in the wind tunnel" when "used vertically and in the appropriate length". He however also acknowledges the main disadvantage of HWA, being its natural insensitivity to angular changes in the velocity vector normal to the wire axis (e.g., [36,38]). Because of this, measurements are limited to flows of low to moderate turbulence intensities. Flow reversal at high turbulence intensities can strictly not be measured by single-wire probes. In this respect, Durgin [38] states that for very high turbulence levels (e.g. larger than 20% when the actual wind may reverse itself), HWA will rectify the negative wind and indicate too high an average and too low a root mean square variation (rms) about the average, but that it will however indicate the correct peak 3 second gust when the appropriate filter is used in the output. Other disadvantages of HWA are its fragility, the fact that it can only be used in clean gas flows, its sensitivity to ambient temperature change and the requirement of frequent recalibration due to dust accumulation.

The use of HWA for PLW studies has been reported by – among others – Wise [1], Penwarden and Wise [98], Wiren et al. [99], Murakami et al. [100], Kamei and Maruta [24], Kawamura et al. [27], Lam [29], White [101], Livesey et al. [46,47], Uematsu et al. [30], Yamada et al. [50] and Sasaki et al. [52].

2.2. Hot- film anemometry

Only single-film measurements as commonly used in PLW studies are addressed. HFA uses a 1 to 5 μm thick conducting film that is deposited on a ceramic cone-, wedge-, or cylinder-shaped substrate, e.g. a platinum film on the surface of a quartz rod with a typical diameter of 25-50 μm (Fig. 2b). For PLW studies, the single film should be positioned vertically in the wind tunnel, to measure the horizontal wind components and provide an average speed over the film length.

Advantages of HFA compared to HWA are the use of a shorter sensing length, lower fragility, more flexibility in sensor configuration, lower susceptibility to fouling and easier to clean. The main disadvantage of HFA is the same as for HWA: the insensitivity to angular changes in the velocity vector normal to the wire axis and the resulting incapability to measure flow reversal. HFA has a lower frequency response than the HWA (about 100 Hz) which however is considered adequate for PLW studies [4,5,91].

The use of HFA for PLW studies has been reported by – among others – Isyumov and Davenport [23], Isyumov [102], Stathopoulos [25], Stathopoulos and Storms [26], Ratcliff and Peterka [28], Jamieson et al. [31]), Wu and Stathopoulos [39,51,91] and Blocken et al. [32,33].

2.3. Pulsed-wire anemometry

As mentioned above, the main disadvantages of HWA and HFA are that flow reversal at high turbulence intensities can strictly not be measured by single-wire probes. This can be circumvented by multi-wire probes and complex data analysis [36], which however are not commonly employed for PLW studies. Another alternative is Pulsed-Wire Anemometry (PWA) that measures the fluid velocity by timing the passage of a heat tracer between two fine wires (Fig. 3) [34,36, 103-105].

Castro [36] provided a detailed overview of advantages and disadvantages of PWA. PWA is especially useful in flows of high turbulence intensity and has therefore been used to greatest effect in separated flows [36,103]. Because typical PWA probes are significantly larger than HWA probes (although the wire spacing is similar to standard hot-wire lengths), PWA is best used in relatively large-scale experiments. This minimizes the problems related to the intrusive character of the technique and it also minimizes the errors arising from velocity shear effects, which are important in near-wall regions [36]. Disadvantages are that the velocity probe head (with wire lengths of about 5 to 10 mm) is quite large compared to standard HWA so that small-scale experiments are difficult, that it should only be used in isothermal flows and that the wires are very delicate, so the probes require much more careful handling than standard HWA probes [36].

The use of PWA for PLW studies has been reported by Britter and Hunt [35].

2.4. Laser-Doppler anemometry

Whereas HWA, HFA en PWA are intrusive techniques, where the probe and probe supports interfere with the flow field, LDA is generally considered to be a non-intrusive technique. This is correct if the seeding of the flow is not considered as flow intrusion. Seeding particles should be small and should have a density similar to that of the ambient fluid. LDA or Laser-Doppler Velocimetry (LDV) uses the Doppler shift in a laser beam to measure the flow velocity. Two crossing beams of collimated, monochromatic and coherent laser light generate a set of

straight fringes (Fig. 4). Seeding particles in the flow that pass through the fringes scatter light that oscillates with a specific frequency that is related to the velocity of the particles.

Advantages of LDA are its non-intrusive character, the high spatial resolution, its directional sensitivity which allows measuring high-turbulence intensity flow and the fact that the measurement is independent of the thermophysical properties of the ambient fluid. It is also suitable for measuring very low velocities as opposed to HWA, HFA and PWA that introduce thermal convection in the flow. Disadvantages are the relatively high cost (compared to HWA, HFA and PWA), the requirement for seeding the flow (if the flow does not already contain seeding in itself) and the need for careful alignment of the beams. The type of seeding also limits the actual time resolution of the flow that can be measured, as the seeding particles do not follow the highest frequencies of the flow field.

The use of LDA for PLW studies has been reported by – among others – Bottema [56], Wu and Stathopoulos [51] and van Beeck et al. [41].

2.5. Irwin probes

Irwin [37] developed and presented a simple omnidirectional sensor, specifically devised for wind-tunnel studies of PLW (Fig. 5), which was later termed "Irwin sensor" or "Irwin probe" (by e.g. Durgin [38], Monteiro and Viegas [40], van Beeck et al. [41]) or Surface Wind Sensor (SWS) (by e.g. Williams and Wardlaw [106], Wu and Stathopoulos [39]). The Irwin probe consists of a hole of diameter D in the model street surface with in its center a protruding tube of external diameter d slightly less than D. The tube protrudes to a height h above the street surface and the top of the tube is flat. Irwin [37] noted that experiments indicated there is little to be gained by using more complex shapes. The excess pressure Δp at the bottom of the sensor hole over that at the top of the sensor tube is measured and from this pressure difference the wind speed at a chosen height h_s above the surface is calculated using a calibration formula, by assuming that the top of the probe is in the log-law dominated part of the boundary layer, as in the calibration experiments which are typically performed in an empty wind tunnel.

The main advantage of the Irwin probe, as mentioned by Irwin [37] himself, is that it allows measurements of PLW speed rapidly at a large number of locations. Indeed, the axi-symmetry of the sensor avoids the need for adjustments or re-alignments each time the wind direction (i.e. rotation of the turntable with model) is changed. It should be noted however that this is also the case for omnidirectional HWA or HFA. Regardless, the Irwin probe is very robust and easy to use: it is less fragile, less susceptible to fouling and much easier to clean than hot wires or hot films. Disadvantages of the Irwin probe however are, just as for HWA and HFA, its directional insensitivity to angular changes in the velocity vector in a horizontal plane and the resulting incapability to measure flow reversal. In addition, the calibration formula assumes that the top of the tube is in the logarithmic law-of-the-wall region, which may not be the case for all areas of the flow field.

Further analysis of the Irwin sensor was performed by Wu and Stathopoulos [39], who analyzed the sensor by comparison with results from HFA. Their findings indicated that the sensor should be set at the same height as the measuring level of the wind speed for a reliable measurement, because considerable errors can result when a short sensor is used to measure the wind flow at a higher level above the ground. They also mentioned that high turbulence intensity may also be a source of error in measurements by HFA and other instruments, and that therefore it is hard to evaluate the Irwin sensor only from the comparison with the vertical HFA data.

The use of Irwin probes for PLW studies has been reported by – among others – Irwin [37], Durgin [38], Williams and Wardlaw [106], Wu and Stathopoulos [39], van Beeck et al. [41] and Tsang et al. [42].

2.6. Scour techniques

Scour techniques refer to the examination of erosion/scouring patterns of a particulate and cohesionless material created by wind flow where a few layers of the particulate material are initially covering the wind-tunnel turntable. Often, sand is used, although also other granular or flaky cereal materials have been tested. Because sand is most often used, in this paper we will use the term "sand-erosion technique" to refer to this type of techniques. The technique originated from studies of snow drifting and snow control in water flumes and tunnels (Theakston, as cited by Livesey et al. [46]). The execution of the sand-erosion technique consists of two stages, as schematically depicted in Figure 6. In the first stage (calibration stage), the wind-tunnel turntable (without building model) is sprinkled with a uniform fine layer of dried sand. Let U_{WT} denote the wind-tunnel speed that is set by the operator of the tunnel (e.g. the speed of the fan). U_{WT} is increased in steps until at a certain wind speed value ($U_{WT,E}$) the sand is blown away. This wind speed represents the erosion speed in free-field conditions. In the second stage, the building model is placed on the turntable and the floor is sprinkled again with a uniform thin layer of sand. Again, the wind-tunnel speed is increased in steps ($U_{WT,1}$, $U_{WT,2}$, . . .) and the sand erosion that occurs locally at each step is allowed to reach a steady state. The areas in the flow field where sand is eroded, are then registered by photography [43-45,90] or digital imaging [47]. From this information, an

estimate of the local amplification factor at the edges of the sand erosion patterns is given by the ratio $K = U_{WT,E}/U_{WT,1}$. The local amplification factor is defined as the local wind speed divided by the wind speed that would occur at the same location if the buildings were absent. Where the sand erodes for a free-stream speed lower than the reference speed, ($U_{WT,1} < U_{WT,E}$), the presence of the building(s) creates a local speed-up ($K > 1$). The locations that are not eroded for $U_{WT,1} > U_{WT,E}$ are locations where the presence of the building(s) creates a local speed-down ($K < 1$). Photographs for successive wind speed intervals can thus be used to draw zones of equal amplification factor, resulting in sand-erosion contour plots, as shown in Figure 7b. This way, it appears that quantitative information can be obtained.

The advantages of the sand-erosion technique are that it is simple, fast and inexpensive. In addition, it has a strong visual character and it provides information over the whole surface area under investigation. This avoids the problem with discrete sensors that there is always a chance that significant problem areas are missed. The strong visual character of sand erosion also aids in the communication of results to building designers, architects and urban planners. Livesey et al. [47] state that the scour technique is ideal for providing information on the "before" and "after" cases, from which an initial assessment of the impact can be made. Disadvantages however are the low measurement accuracy in high-turbulence intensity regions of the flow. In these regions, the sand erodes for a lower mean friction velocity due to large fluctuations around the mean that are higher than the so-called threshold friction-velocity of the sand (U^*_{thr}). Another problem is the easier entrainment of particles due to up-wind particle impacts, also called “down-wind erosion” [49,107]. Sand erosion also has no directional sensitivity and sand erosion tests can depend on the size and geometry of the particles and on the way in which the particle layers are prepared.

A very extensive set of sand-erosion tests was performed by Beranek and Koten [43,44] and Beranek [45,90] on behalf of the Dutch Foundation Building Research *(Stichting Bouwresearch).* The results are reported in an introductory paper [43] and in two extensive reports, one focusing on isolated buildings [44] and one on multi-building configurations [45]. The tests were conducted in a boundary-layer wind tunnel with an approach-flow mean wind speed profile with power-law exponent 0.28 and with buildings at a scale of 1:500. The sand was composed of grains of diameter 0.1-0.2 mm and the thickness of the sand layer was about 0.4 mm. Each wind-tunnel run lasted 2 minutes. Beranek and van Koten [44] reported an excellent reproducibility of the sand-erosion contours. Their documents provide a very large database of information. One of these results is illustrated in Figure 7b. Unfortunately however, apart from the power-law exponent, no information is provided about the approach-flow characteristics of the simulated atmospheric boundary layer, which limits the applicability of the results.

At the Von Karman Institute (VKI) for Fluid Dynamics in Sint-Genesius-Rode, Belgium, sand erosion is a frequently used technique for the assessment of PLW. The calibration is performed on a smooth flat plate. The sand placed on the surface has the property to erode at a given friction velocity, i.e. the threshold friction velocity U^*_{thr}. Erosion is allowed to last 1 minute, which is long enough so that the sand contours are stable and do not depend much on the initial sand thickness non-uniformities and short enough so that extreme gusts do not play and important role [41,49]. The wind-tunnel speed is increased in steps and at each step, a picture is taken. At each step, at the sand contour, the friction velocity is U^*_{thr}. The relationship between sand-erosion patterns and the friction velocity is still not completely understood, especially in separation regions that are characterized by high turbulence levels. The threshold friction velocity is a property of the sand. To extract quantitative data such as wind amplification factors, van Beeck et al. [41] presented a different approach than that reported above. They use the knowledge of the threshold friction velocity to compute the velocity at height z with the universal law of the wall for turbulent flow over a smooth wall [108]:

$$U(z) = U^*_{thr}\left(5 + 2.5\ln\left(\frac{z\,U^*_{thr}}{\nu}\right)\right) \tag{1}$$

where U(z) is the velocity at height z and ν is the kinematic viscosity of air.

The use of scour techniques for PLW studies has been reported by – among others – Cheung [109], Beranek and van Koten [43,44], Borges and Saraiva [110], Beranek [45,90], Durgin [38], Isyumov et al. [111], Isuymov and Amos [112], Surry and Georgiou [113], Livesey et al. [46,47], Uematsu et al. [30], Dezsö [107], van Beeck et al. [41] and Conan et al. [49]. This method has also been used extensively for snow dispersion/accumulation measurements when particles simulating snow are also necessary to be modeled in the wind tunnel.

2.7. Infrared thermography

The infrared thermography technique for PLW speed assessment was developed by Yamada et al. [114,115] and Uematsu et al. [116]. Their work was published in the English language journals by Yamada et al. [50] and Sasaki et al. [52]. This technique was also investigated by Wu and Stathopoulos [51]. It is based on the fact that

the heat transfer from a heated body to the flow is closely related to the flow conditions near the body surface. The set-up used in these experiments by Sasaki et al. [52] is schematically depicted in Figure 8. Part of the wind tunnel floor is made of a 12 mm thick acrylic plate and is warmed up by hot water. The building model made of material with low thermal conductivity is placed at the center of the wind tunnel floor. After a statistically steady state of the wind-flow pattern is achieved, the temperature distribution of the floor surface is recorded by infrared thermography and displayed as a thermal image. The relationship between the surface temperature and the wind speed was investigated by a comparison of the experimental results from infrared thermography and wind speed measurements with HWA. The hot wire was placed vertically at a height equivalent to 1.5 m above the ground. It was found that the temperature reduction δT could be correlated with effective wind speed $U_e = U + 3\sigma_u$ in areas of the flow where the amplification factor $K > 1$, although the correlation coefficient was only situated in the range 0.8-0.9. Note that K is defined as before, i.e. the ratio of the local mean wind speed to the wind speed at the same location without buildings present. Wu and Stathopoulos [51] investigated in more detail the ability to establish correlations between temperature reduction and effective wind speed $U_e = U + 3\sigma_u$, as measured by HFA. The HFA was placed vertically at a height equivalent to 2 m from the ground. Instead of K, they use an overspeed ratio R as the ratio of the effective wind speed to the effective wind speed at the same position without buildings present. For the rectangular building models tested, they identified roughly three zones divided by the dashed lines in Figure 9: (1) $R > 1$ and $\delta T > 0$, corresponding to the corner stream zone, where the increase in wind speeds is indicated by both methods; (2) $R < 1$ and $\delta T > 0$, the frontal-vortex zone, where the results suggested by the two methods are contradictory; and (3) $\delta T < 0$, the wake-turbulence zone, where the sheltering effect is present to some extent. The contradictory results in zone 2 were correctly attributed the important contribution of the vertical velocity component in the downflow to the cooling of the surface. This was confirmed by 3D LDA measurements [48]. In zone 3, it was shown that the wind velocity vector was strongly dominated by its horizontal constituents.

Wu and Stathopoulos [51] provided an overview of the advantages of infrared thermography. In contrast to sand erosion, it is a non-intrusive area technique as it does not require that extra materials are introduced into the measurement. In contrast to sand erosion, only one wind speed is required for a high resolution of temperature distributions. The technique can also be fully computerized and is convenient for data acquisition, processing, and presentation. It is possible to obtain informative statistics such as root-mean-square, peak and spectrum values of the reduced temperature and hence the wind speed, using continuously recorded thermal signals. It should be noted however that this may be impeded by the response dynamics of the heated plate to the surface turbulence with a wide range of fluctuating frequencies. A potential disadvantage is the disturbance of the wind flow by convection, which would constitute some intrusive character of this technique, but Wu and Stathopoulos [51] state that the temperature difference between the measurement plate and air flow can be set at a very low level so that the disturbance to wind flow from the heat convection becomes negligible. Furthermore, it is possible to conduct the tests at high wind speed so the Richardson numbers remain sufficiently low. Like sand erosion, also the infrared thermography technique is easily understandable for building designers and urban planners.

In spite of these advantages, infrared thermography is only very rarely applied for practical PLW assessment. This could be attributed to the main limitations of this technique: the more complicated and non-standard experimental set-up with its different components (Fig. 8) and, maybe most important, the problems in relating the temperature decrease to an effective wind speed. The latter problem is twofold: first, the overall low correlation between temperature decrease and effective wind speed; even in areas with $K > 1$, e.g. corner stream areas, the correlation is only 0.8-0.9, as shown by Yamada et al. [50]; second, the influence of down-flow yielding a strong vertical component in the 3D velocity vector. As discussed by Wu and Stathopoulos [51], this component is not detected by HFA but contributes significant to the temperature decrease. It should be noted that the vertical component of the wind velocity vector might be perceived as causing discomfort but it does not act to destabilize pedestrians.

2.8. Particle image velocimetry

PIV is generally considered to be a non-intrusive area technique. This is correct if the seeding of the flow is not considered as flow intrusion, i.e. when the particles are sufficiently small and their density is similar to that of the ambient fluid. Tracer particles in the flow are illuminated by two short pulses of a laser sheet and these illuminations are recorded on camera (Fig. 10). As such, also the motion of these particles is recorded. The local velocity is then estimated from the displacement of these particles (actually groups of particles) over the short time interval between the two pulses.

Advantages of PIV are its non-intrusive character, its high spatial resolution, its directional sensitivity and the fact that it is an area technique. Despite the very good spatial resolution, the frequency resolution of PIV is often a limitation for measuring the turbulence spectra (> 10 kHz needed) that is an order of magnitude above the classical PIV possibilities [49], although this is not considered a disadvantage for PLW studies. Furthermore,

laser-light shielding and/or reflections by buildings in multi-building models can seriously hamper the successful application of PIV. This is especially problematic for PLW problems which typically involve clusters of buildings [70].

PIV studies for PLW have only been published by Deszö [107], van Beeck et al. [41] and Conan et al. [49].

2.9. Other techniques

For completeness some other techniques are briefly mentioned here. Other point techniques include thermistors (i.e. sensors similar to hot-wire or hot-film anemometers but without their high frequency response to measure gust speeds), the Preston sensor (similar to the Irwin sensor), the Pitot static tube [107,117], the deflection velocimeter [118] and the sonic flowmeter [119]. Another area technique is oil streaking [44] that provides spatially continuous information of the local surface shear stress and therefore an indication of surface wind speed (Fig. 7c). Other visualization techniques that can be used to provide a qualitative indication of the flow include smoke streaklines, particle injection, tufts and directional vanes.

3. Accuracy of wind-tunnel techniques for pedestrian-level wind speed

Acknowledging the fact that it is difficult to determine the absolute accuracy of a particular wind-tunnel technique in a given situation, this section will present comparisons between various techniques, as reported in the literature.

3.1. Comparison between HFA and on-site measurements

Isyumov and Davenport [23] compared wind-tunnel measurements and full-scale measurements of mean wind speed for the Commerce Court Plaza project in Toronto, Canada. The wind-tunnel measurements were performed with single-ended hot-film anemometer probes. The full-scale measurements of wind speed and wind direction were made with a propeller vane anemometer mounted on a portable tripod. The comparisons were made for 7 plaza locations, where the full-scale measurements were conducted sequentially at each location twice a day during a two-week period. Although Isyumov and Davenport [23] acknowledged that the two-week period was not adequate to allow a comprehensive comparison, they reported that the agreement between wind-tunnel and full-scale mean wind speed was particularly encouraging for relatively windy areas of the plaza, where it was found to be within about 10%, as shown in Figure 11. They concluded that this 10% agreement was encouraging because it implied that representative wind tunnel methods can effectively provide information on the more important aspects of the surface wind speed climate [23].

3.2. Comparison between scour tests and HWA

Many factors influence the accuracy and reliability of quantitative information derived from scour tests. Livesey et al. [46] in their first journal paper on scour techniques indicate some particular difficulties in obtaining quantitative data from scour tests, including the fact that turbulence in the flow promotes an earlier particle motion and increases the rate of transport. Therefore, they mention that the observed initial scour patterns might be related to some measure of the instantaneous rather than the mean wind speed. From this study, they concluded that these data are most suited for describing less quantitative measures of the wind environment where relative rather than absolute information is needed. Later, Durgin [38] labeled the results from scour tests as semi-quantitative. In 1992, Livesey et al. [47] reported a continued and more detailed evaluation of scour tests by comparison with HWA at the Boundary Layer Wind Tunnel Laboratory (BLWTL). Based on this work, they concluded that the scour technique can now be a useful tool for quantifying the extent of the impact of a new development on its surroundings [47].

The information below briefly reports how they arrived to this conclusion. The scour tests were performed with a bran, the particles of which are plate-like and light, rather than granular, as sand. First, in the calibration stage, the threshold wind speed of the particulate material was determined. To this extent, the empty wind tunnel turntable was covered with a thin uniform layer of the material, a few grains deep, and the wind tunnel speed was increased until steady-state scouring is achieved. The exact speed at which particle movement occurs was rather difficult to determine due to the variability of the surface characteristics and the influence of turbulence. Therefore, the calibration procedure was repeated several times and an average of the threshold wind speed values was taken. Next, in the actual testing stage, tests were conducted for a block of L x W x H = 0.1 x 0.1 x 0.2 m³ in an atmospheric boundary layer wind tunnel, for wind angles 0° and 45°. From the threshold wind speed of motion of the material, several wind speed-up ratios or amplification factors were chosen: K = 0.8, 1.0, 1.2, 1.4, 1.6, 1.8, 2.0. These factors were defined as the ratio of the threshold wind speed to the actual test wind speed. At each of these amplification factors, the wind tunnel was run for two minutes to reach a steady-state

scouring pattern. After every test, a photograph was taken of the scour patterns. The scour tests were compared to HWA to determine what kind of wind speed is actually measured by the scour technique and how these estimates compare to those of a so-called more "quantitative" method. HWA was conducted with a dense grid of 224 omnidirectional (vertically-oriented) HWA positions: upstream, besides and downstream of the block. The results were presented as the ratio of the mean wind speed at pedestrian level to the mean wind speed at gradient height, V_i/V_h. Figure 12 compares the scour test and HWA results by plotting the ratio $(V_i/V_h)_{scour}/(V_i/V_h)_{HWA}$ as a function of $(V_i/V_h)_{HWA}$. Livesey et al. [47] reported that the agreement between wind speed ratios obtained from scour tests and HWA depends on the magnitude of the turbulence intensity in the area of interest, relative to that at the test location at which the threshold speed of the material has been determined. When the turbulence intensities are comparable, as they were in this study, the scour patterns provide an indication of the local mean wind speed, so with a peak factor k = 0. This is the mean wind speed which is used to describe the threshold speed in the calibration of the material. Livesey et al. [47] however also state that different shapes, densities and particle sizes of materials may give different results for comparisons with HWA speeds. Note that Figure 12 clearly shows that the deviations between scour tests and HWA measurements decrease rapidly with increasing ratio $(V_i/V_h)_{HWA}$. In other words, scour tests and HWA give very similar results for high wind speed areas.

3.3. Comparison between sand erosion and PIV

Detailed wind-tunnel experiments with sand-erosion tests and PIV were performed at the VKI in Sint-Genesius-Rode, Belgium, for a backward facing step (BFS) (Fig. 13) [41,49,107]. In spite of its geometrical simplicity, the two-dimensional backward-facing step is a useful geometry for testing in building aerodynamics because the flow contains most of the salient features that are also present in the flow around buildings: flow separation, a shear layer, a recirculation zone (near wake), an impingement zone and a far wake. The experiments were conducted in a small low-speed blowing type wind tunnel with a test section of 0.2 x 0.2 m². The tunnel was equipped with a 1000 mm long wooden flat plate with the height of the BFS H = 20 mm (Fig. 13a). Upstream of the BFS the test section is reduced to 0.20 x 0.18 m². The BFS height was 2.00 +/- 0.01 cm and the radius of curvature of the step edge is 0.1 mm. The aspect ratio of the step is 10. The transition of the boundary layer was triggered at the leading edge of the plate by a 0.1 m fetch of rough emery paper (Fig. 13b). The flow is characterized by Re_H based on the step height of 21,800, where U_∞ = 17.1 m/s is the free-stream velocity upstream of the step. This Re number is well above the critical value of 11,000 that is often used as a threshold for Reynolds-number independent flow for bluff bodies with sharp edges [120]. First, PIV was used to measure the velocity vector field downstream of the BFS. The PIV measurements were made in the vertical center plane. A set of 500 images was used for computing the time-averaged velocity field, which is shown in Figure 14. The estimated single-velocity measurement error is approximately 0.25 m/s [49]. Next, the sand erosion tests were performed. The calibration for the sand erosion tests was performed on a smooth flat plate, also equipped with an emery paper strip, to determine the free-stream wind speed U_∞ at which sand erosion occurs. For the actual tests, the downstream part of the step was covered with a thin layer of sand (Fig. 13b) and the amplification factor K was computed for five free-stream velocities U_∞ = 15.3, 16.0, 16.5, 17.0 and 17.6 m/s. The sand erosion and PIV results are compared in Figure 15a. Figure 15b shows the sand layers downstream of the BFS after 1 minute for a free stream velocity of 17 m/s. Sand remains in the low velocity regions, i.e. the small corner vortex and the reattachment zone of the large recirculation bubble near X/H = 6 (see Fig. 14b). For the PIV results in Figure 15a, two curves are given: one for the mean wind speed U and one for the mean wind speed plus the rms value. The sand erosion results exhibit the same trend as the PIV measurements and are situated between the two PIV curves. For low turbulence areas (x/H < 3), sand erosion provides a very good agreement (within 2%) with the mean wind speed PIV results, while in the high-turbulence reattachment area (4.5 < x/H < 6.5) the sand erosion results are closer to $U + U_{rms}$. The sand erosion results overestimate the mean velocity in areas with high turbulence intensity. This is in line with the findings from Livesey et al. [47] described in the previous section. As in the previous comparison study, the conclusion is that scour tests – when conducted carefully – can provide an accurate quantitative estimate of the mean wind speed in areas of high mean wind speed U and hence high amplification factor (which are the areas where the turbulence intensity σ_u/U is low).

3.4. Comparison between sand erosion and LDA

Comparisons between sand erosion and LDA were performed by van Beeck et al. [41]. For this comparison, quantitative values of the mean wind speed (not amplification factor or any other wind speed ratio) were obtained from the sand-erosion tests using the procedure presented by van Beeck et al. [41] that is based on the logarithmic law of the wall (Eq. 1). Sand grains with a maximum diameter of 600 micrometer were obtained by sieving. A 1-2 mm thick sand layer was spread on the wind-tunnel floor. For the sand used, the friction velocity U^*_{thr} = 0.23 m/s. The calibration for this critical friction velocity has been carried out on a smooth flat plate using a flattened pitot tube for the velocity profile, post-processed by Bradshaw's method [117] to obtain the

friction velocity at the moment sand starts to erode in reptation mode [107], such that the moving sand grains do not have enough energy to induce secondary erosion due to sand impingement. At each step, at the borders of the erosion patterns, the velocity is the friction velocity. From the logarithmic law of the wall [121] and the value of U^*_{thr} the mean velocity profile is given by Eq. (1). This value is about 5 m/s at 10 mm above the wind tunnel floor, which corresponds to about 1.75m in reality if the model scale would be 1:175. Note that 5 m/s is also the threshold mean velocity used in the Dutch standard for wind comfort assessment [19]. Eq. (1) might lead to a too high mean velocity estimation if the photograph of the sand erosion patterns is taken after 1 minute. In reality sand erosion will also occur at locations with a low mean wind velocity and a high probability of gusts [107,122]. Figure 16 depicts the comparison between the velocity magnitude deduced from the sand erosion technique in combination with Eq. (1) and from LDA as a function of X/H for different distances from the floor, i.e. until 1/4th the BFS step height. For the sand erosion technique, the velocity is deduced from Eq. (1) at locations where the BFS-centerline crosses the three visible sand contours. The mean velocity deduced from the sand erosion technique is overestimated by less than 10% with respect to the LDA mean wind speed in the recovery region. In the recirculation region, the overestimation is more than 20% due to turbulence/gusts, getting worse further away from the sand layer, where the applicability of Eq. (1) fails. Note that only in the recovery region in the far wake (x/H = 7.5), the variation of the wind speed with height is correctly predicted by sand erosion in Eq. (1), indicating that the log law is only valid at these positions.

3.5. Comparison between Irwin probes and LDA

Comparisons between Irwin probes and LDA for the same BFS as in previous subsections were presented by van Beeck et al. [41]. Five Irwin sensors were placed (Fig. 17a): one in the small corner vortex, two in the large recirculation zone, one near the reattachment point and one in the recovery region. For every position, Irwin probe and LDA measurements were made at five heights: 1, 2, 3, 4 and 5 mm. Figure 17b shows that the Irwin probes overestimate the wind speed by up to more than a factor 2 in locations with a mean velocity below 1.5 m/s. Overestimations drop below 20% above 3 m/s in the recirculation zone. In the recovery region after the reattachment point, the mean velocity from the Irwin probe deviates less than 5% with respect to the LDA mean velocity. The conclusion made from this comparison is that the Irwin probes can provide accurate results of mean wind speed in the area of high wind speed / low turbulence intensity.

3.6. Comparison between Irwin probes and HFA

Wu and Stathopoulos [91] compared results from Irwin probes and HFA for a 1/400 scale model of a rectangular high-rise building (Fig. 18). The Irwin probes had 5 mm height and were installed at 37 positions. Later, vertically installed hot films with their center at 5 mm above the tunnel floor measured mean and RMS wind speed at 42 positions. Figure 18 indicates a close agreement between the two measurement sets in the upstream area and the corner stream regions. In the near wake behind the building, the Irwin probe provides higher mean speed ratios than HFA. Again, the agreement between the techniques is good to very good in the areas of high wind speed U and hence high amplification factor K.

3.7. Observations and/or statements from other comparative wind-tunnel studies

Visser and Cleijne [123] refer to four studies [23,27,124,125] in which comparisons of wind-tunnel measurements with HWA or HFA and full-scale data were made. All these studies concerned high-rise buildings and the agreement ranged from moderate to quite good, with the best agreement for the windiest locations, i.e. those with the highest amplification factor K.

The VKI successfully extended the use of the sand-erosion technique beyond the application of PLW. Sanz-Rodrigo et al. [126] applied this technique to study snow drift (removal and accumulation) around the new Belgian Antartic base, where this technique proved very valuable to determine not only the optimal position but also the orientation of the station. Conan et al. [49] applied the sand-erosion technique to estimate wind speed over mountainous terrain, aimed at wind resource assessment for wind energy applications (Fig. 19). They reported that for high speed positions, results extracted from sand erosion appeared to be comparable to those calculated by PIV, and that the technique is repeatable, able to perform a detection of the high speed area and capable of giving an estimate of the amplitude of the wind.

Comparisons between infrared thermography and HWA were made by Yamada et al. [50] and Wu and Stathopoulos [51]. As already mentioned in section 2.7, these comparisons indicated the difficulty in relating the surface temperature reduction to an effective wind speed, also in areas with high amplification factors such as the standing vortex in front of the building.

3.8. Remark

The large number of previous studies outlined above systematically indicate that the lower-cost techniques HWA, HFA, Irwin probes and sand erosion provide quantitative results very close to those by the higher-cost and more accurate techniques LDA and PIV, at least in the so-called "windiest" areas, which are the areas with high amplification factor. These are precisely the areas where the assessment of wind comfort is most important. An exception is infrared thermography, where HWA indicates very different results in the standing vortex.

4. Best practice guidelines for wind-tunnel testing of pedestrian-level wind speed

In 1975, Isyumov and Davenport [23] published their pioneering study of comparing full-scale and wind-tunnel wind speed measurements in the Commerce Court Plaza in Toronto. At the end of this study, they mentioned that a representative simulation of the overall full-scale flow regime is a prerequisite to effective wind tunnel assessments of the flow around and within building complexes, based on their experience that pedestrian level flow conditions even in a very built-up environment are quite sensitive to the structure of the approaching wind [23]. They concluded that, in boundary layer wind tunnel simulations, it is important to representatively model both the immediate proximity of the area of interest as well as the structure of the approaching flow [23].. Indeed, if best practice is not applied to the structure of the approaching flow, accurate results cannot be expected, irrespective of the measurement technique. It is therefore not surprising that the best practice advice published in the ASCE Manuals and Reports on Engineering Practice No. 67: Wind Tunnel Studies of Buildings and Structures [4] focuses in depth on characteristics of ABL wind tunnels, on wind-tunnel modeling of the ABL, on the generation of topographic models, on the influence or near-field and specific structures, on the selection of the geometric and velocity scale and on Reynolds number scaling. For more information, the reader is referred to these documents.

Once the adequacy of representation of the structure of the approaching flow is ensured, the focus can shift to the selection of an appropriate measurement technique. Irwin [89] stated that it may be worth using a less accurate measuring system if it results in an improved coverage. Wu and Stathopoulos [91] mentioned that a suggested approach might consist of two stages: first to use area methods (such as scour tests or infrared thermography) for assessing the wind behavior and identifying windy zones in a wide area, next to carry out point measurements (such as HWA, HFA, Irwin probe measurements or LDA) for detailed information at some critical positions. This suggested approach originates from the stronger quantitative features of the so-called point methods as opposed to scour test or infrared thermography. ASCE [5] states that the choice of experimental technique must be guided by the requirements for accuracy, repeatability, stability, resolution and cost. Measurements must sample the wind for a sufficient time to obtain statistically stable values of the target variables. The number of measurement locations depends on the extent of the model area to be covered and on the type of instruments used. HWA could typically use 20 to 40 locations, but with Irwin sensors more locations are feasible, e.g. 50 to 100, or even more [104,127].

5. CFD techniques for pedestrian-level wind speed

As illustrated by a detailed review of 50 years of computational wind engineering [82], CFD is gaining increasing acceptance as a tool for PLW studies. This can to a large extent be attributed to the support by the increasing number of best practice guidelines for CFD that have been published in the past 15 years, many of which were developed with specific focus on PLW [70-73,77,83,128,129]. This increased acceptance has also been confirmed by the publication of the new Dutch Wind Nuisance Standard, NEN8100 [11,19] that specifically allows the user to choose between wind-tunnel testing and CFD for analyzing PLW comfort and safety. CFD has some particular advantages compared to wind-tunnel testing. It provides whole-flow field data, i.e. data on the relevant parameters in all points of the computational domain. As such, CFD can avoid the two-stage process in wind-tunnel testing (first application of area technique followed by application of point technique). Unlike wind-tunnel testing, CFD does not suffer from potentially incompatible similarity requirements because simulations can be conducted at full scale. This is particularly important for extensive urban areas that would require too large scaling factors. CFD simulations easily allow parametric studies to evaluate alternative design configurations, especially when the different configurations are all a priori embedded within the same computational domain and grid. However, the accuracy of CFD is a matter of concern and verification and validation studies are imperative. This concern is also reflected in the Dutch Wind Nuisance Standard that demands quality assurance – it actually does this both for CFD and for wind-tunnel testing. Note that CFD solution verification and validation and complete reporting of the followed procedure are essential components of quality assurance. The following sections briefly address the approximate forms of the governing equations that are most frequently used in wind engineering studies.

5.1. Navier-Stokes equations

The governing equations are the three laws of conservation: (1) conversation of mass (continuity); (2) conservation of momentum (Newton's second law); and (3) conservation of energy (first law of thermodynamics). The energy equation will not be considered in this paper. While strictly the term Navier-Stokes (NS) equations only covers Newton's second law, in CFD it is generally used to refer to the entire set of conservation equations. The instantaneous three-dimensional NS equations for a confined, incompressible, viscous flow of a Newtonian fluid, in Cartesian co-ordinates and in partial differential equation form are:

$$\frac{\partial u_i}{\partial x_i} = 0 \tag{2a}$$

$$\frac{\partial u_i}{\partial t} + u_j \frac{\partial u_i}{\partial x_j} = -\frac{1}{\rho}\frac{\partial p}{\partial x_i} + \frac{\partial}{\partial x_j}\left(2\nu s_{ij}\right) \tag{2b}$$

The vectors u_i and x_i are instantaneous velocity and position, p is the instantaneous pressure, t is time, ρ is the density, ν is the molecular kinematic viscosity and s_{ij} is the strain-rate tensor:

$$s_{ij} = \frac{1}{2}\left(\frac{\partial u_i}{\partial x_j} + \frac{\partial u_j}{\partial x_i}\right) \tag{2c}$$

As directly solving the NS equations for the high-Reynolds number flows in urban physics and wind engineering is currently prohibitively expensive, approximate forms of these equations are solved. Two main categories used in wind engineering are RANS and LES. RANS stands for Reynolds-averaged Navier-Stokes, while LES is the acronym for Large Eddy Simulation. In addition, hybrid RANS/LES approaches exist, although they are only very rarely used in urban physics and wind engineering.

5.2. Reynolds-averaged Navier-Stokes

The RANS equations are derived by averaging the Navier-Stokes (NS) equations (time-averaging if the flow is statistically steady or ensemble-averaging for time-dependent flows). With the RANS equations, only the mean flow is solved while all scales of the turbulence are modeled (i.e. approximated). This is schematically depicted in Figure 20. Up to now, RANS has been by far the most commonly used approach in CFD for PLW.

The RANS equations are obtained by decomposing the solution variables as they appear in the instantaneous NS equations (Eqs. 2a-b) into a mean (ensemble-averaged or time-averaged) and a fluctuation component. For an instantaneous variable φ this means:

$$\varphi = \overline{\varphi} + \varphi' \tag{3}$$

where $\overline{\varphi}$ is the mean and φ' the fluctuating component (around the mean). Replacing the instantaneous variables in Eq. (2a-b) by the sum of the mean and the fluctuation components and taking an ensemble-average or time-average yields the RANS equations:

$$\frac{\partial \overline{u}_i}{\partial x_i} = 0 \tag{4a}$$

$$\frac{\partial \overline{u}_i}{\partial t} + \overline{u}_j \frac{\partial \overline{u}_i}{\partial x_j} = -\frac{1}{\rho}\frac{\partial \overline{p}}{\partial x_i} + \frac{\partial}{\partial x_j}\left(2\nu \overline{s}_{ij} - \overline{u_j' u_i'}\right) \tag{4b}$$

Here, $\overline{u}_i$ and $\overline{p}$ are the mean velocity and mean pressure, u_i' and p' are the fluctuating components and $\overline{s}_{ij}$ is the mean strain-rate tensor:

$$\bar{s}_{ij} = \frac{1}{2}\left(\frac{\partial \bar{u}_i}{\partial x_j} + \frac{\partial \bar{u}_j}{\partial x_i}\right) \quad (4c)$$

The horizontal bar in the equations denotes averaging. When comparing the set of equations (Eq. 4) with the instantaneous set (Eqs. 2), the similarity between both sets is observed, but also that the averaging process has introduced new terms, which are called the Reynolds stresses or turbulent momentum fluxes. They represent the influence of turbulence on the mean flow. The instantaneous NS equations (Eqs. 2) form a closed set of equations (four equations with four unknowns: u_i and p). The RANS equations do not form a closed set due to the presence of the Reynolds stresses and turbulent heat and mass fluxes (more unknowns than equations). It is impossible to derive a closed set of exact equations for the mean flow variables [130]. Closure must therefore be obtained by modeling. The modeling approximations for the Reynolds stresses are called turbulence models.

A distinction has to be made between steady RANS and unsteady RANS (URANS). Steady RANS refers to time-averaging of the NS equations and yields statistically steady descriptions of turbulent flow. URANS refers to ensemble-averaging of the NS equations. URANS only resolves the unsteady mean-flow structures, while it models the turbulence. LES on the other hand actually resolves the large scales of the turbulence. URANS can be a good option when the unsteadiness is pronounced and deterministic, such as von Karman vortex shedding in the wake of an obstacle with a low-turbulence approach flow. However, given the relatively high turbulence in (approach-flow) atmospheric boundary layers, LES or hybrid URANS/LES should be preferred over URANS for these applications. Tominaga [131] provides a thorough discussion of the use of URANS for wind flow around an isolated building, focused on the effect of large-scale fluctuations on the velocity statistics. Franke et al. [72] state that, since URANS also requires a high spatial resolution, it is recommended to directly use LES or hybrid URANS/LES. As shown by a literature review on CFD for PLW but also by a review of other literature reviews on CFD in wind engineering [82], steady RANS is by far most often used, in spite of its deficiencies. Studies that have employed unsteady RANS (URANS) are scarce.

Two main types of RANS closure models can be distinguished: first-order closure and second-order closure models. First-order closure uses the Boussinesq eddy-viscosity hypothesis to relate the Reynolds stresses to the mean velocity gradients in the mean flow:

$$-\overline{u_i' u_j'} = 2\nu_t S_{ij} - \frac{2}{3} k \delta_{ij} \quad (5)$$

where ν_t is the turbulent viscosity (also called momentum diffusivity), k is the turbulent kinetic energy and δ_{ij} is the Kronecker delta:

$$k = \frac{1}{2}\overline{u_i' u_i'} \quad (6)$$

$$\delta_{ij} = \begin{cases} 1 & \text{for } i = j \\ 0 & \text{for } i \neq j \end{cases} \quad (7)$$

In first-order closure, the turbulence models need to provide expressions for the turbulent (eddy) viscosity, and are called eddy-viscosity models. A distinction is made between linear and non-linear eddy-viscosity models. Examples are the one-equation Spalart-Allmaras model [132], the standard k-ε model [133] and its many modified versions, such as the Renormalization Group (RNG) k-ε model [134] and the realizable k-ε model [135], the standard k-ω model [136] and the k-ω shear stress transport (SST) model [137]. Second-order closure is also referred to as second-moment closure or Reynolds Stress modeling (RSM). It consists of establishing and solving additional transport equations for each of the Reynolds stresses and the turbulence dissipation rate.

The use of steady RANS CFD for PLW studies has been reported by – among others – Murakami [53], Gadilhe et al. [54], Takakura et al. [55], Bottema [56], Stathopoulos and Baskaran [57], Baskaran and Kashef [58], Murakami [59], Ferreira et al. [60], Mochida et al. [61], Richards et al. [48], Meroney et al. [62], Miles and Westbury [63], Westbury et al. [64], Hirsch et al. [65], Blocken et al. [33,66,67,70], Zhang et al. [74], Yoshie et al. [75], Mochida and Lun [76], Blocken and Carmeliet [68], Blocken and Persoon [69], Bady et al. [78], Janssen et al. [18], Montazeri et al. [80], Shi et al. [84], Vernay et al. [85], Yuan et al. [138].

5.3. Large eddy simulation

In the LES approach, the NS equations are filtered, which consists of removing only the small turbulent eddies that are smaller than the size of a filter that is often taken as the grid size (Figure 20). The large-scale motions of the flow are solved, while the small-scale motions are modeled: the filtering process generates additional unknowns that must be modeled in order to obtain closure. This is done with a sub-filter turbulence model. The following notation is used for a filtered variable (denoted by the tilde):

$$\tilde{\varphi}(x) = \int_D \varphi(x')\, G(x, x')\, dx' \tag{8}$$

with D the fluid domain and G the filter function determining the scale of the resolved eddies. Often, the grid size is used as the filter. This is schematically depicted in Figure 20.

The LES equations are obtained by decomposing the solution variables:

$$\varphi = \tilde{\varphi} + \varphi' \tag{9}$$

where $\tilde{\varphi}$ is the resolvable part and φ' the subgrid-scale part. Substituting Eq. (9) into Eqs. (2a-b) and then filtering the resulting equation yields the equations for the resolved field, i.e. the filtered NS equations:

$$\frac{\partial \tilde{u}_i}{\partial x_i} = 0 \tag{10a}$$

$$\frac{\partial \tilde{u}_i}{\partial t} + \tilde{u}_j \frac{\partial \tilde{u}_i}{\partial x_j} = -\frac{1}{\rho}\frac{\partial \tilde{p}}{\partial x_i} + \frac{\partial}{\partial x_j}\left(2\nu \tilde{s}_{ij} - \overline{u_j' u_i'}\right) \tag{10b}$$

Here, $\tilde{u}_i$ and $\tilde{p}$ are the resolvable velocity and resolvable pressure, u_i' and p' are the subgrid-scale parts, and $-\overline{u_j' u_i'}$ is the subgrid-scale stress resulting from the filtering operation. $\tilde{s}_{ij}$ is the rate-of-strain tensor for the resolved scale:

$$\tilde{s}_{ij} = \frac{1}{2}\left(\frac{\partial \tilde{u}_i}{\partial x_j} + \frac{\partial \tilde{u}_j}{\partial x_i}\right) \tag{11}$$

As in the RAN S approach, closure in LES needs to be obtained by modeling. The modeling approximations for the subgrid-scale stresses are called subgrid-scale models. Often, the Boussinesq hypothesis is adopted:

$$\tau_{ij} - \frac{1}{3}\tau_{kk}\delta_{ij} = -2\mu_t \tilde{s}_{ij} \tag{12}$$

$$\tau_{ij} = \tilde{u}_i \tilde{u}_j - \overline{u_i u_j} \tag{13}$$

with μ_t the subgrid-scale turbulent viscosity. The isotropic part of the subgrid-scale stresses τ_{kk} is not modeled but added to the filtered static pressure term. To obtain μ_t , different subgrid-scale models have been devised, such as the Smagorinsky-Lilly model, the dynamic Smagorinsky-Lilly model and the dynamic energy subgrid-scale model.

LES is intrinsically superior in terms of physical modelling to both steady and unsteady RANS, simply because a larger part of the unsteady turbulent flow is actually resolved. Therefore, it is very suitable for simulating the turbulent and non-linear nature of wind flow around buildings. In addition, its application is increasingly supported by ever increasing computing resources. However, for many applications including PLW, 3D steady RANS remains the main CFD approach up to the present day, where it is often being applied with a satisfactory degree of success, as shown by a detailed review of the literature in computational wind engineering [82]. To the opinion of the present authors, three main reasons are responsible for the lack of application of LES in PLW studies: (1) The computational cost of LES. This cost is at least an order of magnitude larger than for RANS, and possibly two orders of magnitude larger when including the necessary actions for solution verification and validation. (2) The

increased complexity of LES. It requires an inlet condition with time and space resolved data and appropriate consistent wall functions with roughness modification that can feed turbulence into the flow. In addition, a large amount of output data is generated. (3) The lack of quality assessment in practical applications of LES and the lack of best practice guidelines in LES, which might even lead to a lack of confidence in LES. These arguments are further explained below.

Even without the necessary actions for verification and validation, LES remains very computationally demanding [139], and often too computationally demanding for practical PLW applications, where generally simulations need to be made for at least 12 wind directions [75], and sometimes even more. When the necessary actions of quality assurance are included – as they should – simulations for several of these different wind directions should be performed on different grids and with different subgrid-scale models to ensure the accuracy and reliability of the simulations. This can be done using techniques such as the Systematic Grid and Model Variation technique (e.g. [140-142]). This care for accuracy and reliability is especially important in LES because, as stated by Hanna [143]: *"... as the model formulation increases in complexity, the likelihood of degrading the model's performance due to input data and model parameter uncertainty increases as well.*" This motivates the establishment of generally accepted extensive best practice guideline documents for LES in wind engineering. However, while such guidelines have been developed for RANS in the past 15 years (see section 7), this is not (yet) the case for LES. This is turn can be attributed to the computational expense of LES, as the establishment of such guidelines requires extensive sensitivity tests.

6. Accuracy of CFD techniques for pedestrian-level wind speed

6.1. Steady RANS versus wind-tunnel measurements

Attempts to provide general statements about the accuracy of steady RANS CFD for PLW studies can easily be compromised by the presence of a combination of numerical errors and physical modelling errors in the simulation results. Statements on the accuracy of steady RANS with a certain turbulence model should therefore be based on CFD studies that satisfy the above-mentioned best practice guidelines. A general observation from such steady RANS PLW studies is that the prediction accuracy is a pronounced function of the location in the flow pattern, and therefore of the wind direction. This is illustrated by reference to a few studies below.

In the framework of the development of the AIJ guideline for wind environment evaluation, Yoshie et al. [75] reported validation studies for – among others – an isolated square prism with ratio L:W:H = 1:1:2 (Figure 21). The simulations were performed with steady RANS with the standard k-ε model and with two revised k-ε models: the Launder-Kato k-ε model [144] and the Renormalization Group (RNG) k-ε model [134]. Note that the simulations included a grid-sensitivity analysis, careful application of the boundary conditions, higher-order discretization schemes, a complete report of the computational settings and parameters and a detailed comparison with the wind-tunnel measurements, all of which are required in order to support the validity of the conclusions. Comparison of the standard k-ε model results with the wind-tunnel measurements showed that the amplification factor $K = U/U_0$ (ratio of local mean wind speed U to the mean wind speed U_0 at the same position without buildings present) is generally predicted within an accuracy of 10% in the regions where $U/U_0 > 1$ (see Fig. 22). In the wake region behind the building however, where $U/U_0 < 1$, the predicted wind speed is generally significantly underestimated, at some locations by a factor 5 or more (Fig. 22). The results of the other turbulence models showed a slight improvement in the high wind-speed regions, but worse results in the wake region. The underestimations in the wake region are attributed to the underestimation of turbulent kinetic energy in the wake, due to the fact that steady RANS is evidently not capable of reproducing the vortex shedding in the wake of buildings [75,145].

Similar conclusions on the different performance in high versus low wind speed regions around buildings were found in the CFD study by Yoshie et al. [75] for the actual urban area in Niigata: in high wind speed regions, the predictions are generally within 20% of the measurements, while the wind speed in low wind speed regions is generally significantly underestimated, at some positions with a factor 5 or more. The comparisons for yet another configuration, the Shinjuku sub-central area, confirmed the findings for the other configurations. While for all their studies, large discrepancies were found in the low wind speed regions, it should be noted that the high wind speed regions are those of interest for pedestrian-level wind studies. In these regions, steady RANS was shown to provide a good to very good accuracy (10-20%).

Blocken and Carmeliet [68] performed steady RANS CFD simulations with the realizable k-ε model [135] for three configurations of parallel buildings and compared the results with the sand-erosion wind-tunnel experiments by Beranek [45]. Three of these comparisons are shown in Figure 23, yielding observations that are very similar to those by Yoshie et al. [75]: a close to very close agreement between CFD and wind-tunnel measurements in the region of high $K = U/U_0$ (about 10% accuracy) and significant underestimations in the regions of lower K. The regions of high K are the corner streams and the areas between the buildings in which pressure short-circuiting occurs [68]. Other results from the same study (not shown in Fig. 21) indicate that also

the high K in the standing vortex is predicted with good accuracy by steady RANS CFD. Note that the standing vortex is only clearly visible for wind directions that are almost perpendicular to the long building facade. Regions of low K do not only occur in the wake of the buildings, but are also found in the low-speed stagnation zone upstream of the buildings. Similar to the results by Yoshie et al. [75], the underestimations in these regions can go up to a factor 5 or more. Note that also these simulations were based on grid-sensitivity analysis, careful application of the boundary conditions and higher order discretization schemes. It should be noted that sand-erosion measurement results are generally considered to be less suitable for CFD validation, although in this study the validation was focused on the region with high K where sand erosion can yield accurate results, as outlined in section 3 of this paper.

Later, similar observations of good steady RANS predictions in regions of high K were reported by Yim et al. [146] and An et al. [147].

6.2. Steady RANS versus on-site measurements

For assessing the accuracy of CFD for PLW studies, it is important to compare them not only with wind-tunnel measurements – where the boundary conditions are generally well-known – but also with well-reported on-site measurements. However, CFD PLW studies in complex urban environments including a comparison with on-site measurements are very scarce. To the knowledge of the author, only four such studies have been published: the study by Yoshie et al. [75] for the Shinjuku Sub-central area in Tokyo, the study by Blocken and Persoon [69] for the area around the multifunctional ArenA stadium in Amsterdam and the studies by Blocken et al. [70] and Janssen et al. [18] for the Eindhoven University campus. Although these measurements were quite limited, overall, the comparisons confirmed the conclusions made earlier, albeit the discrepancies in the high wind speed regions can slightly exceed 10%.

6.3. LES versus steady RANS

To the best knowledge of the authors, comparative studies of LES versus steady RANS focused on PLW have not yet been reported in the open literature. Nevertheless, quite a few studies in building aerodynamics have compared results from LES with those from steady RANS with a variety of turbulence models. Extensive studies by Murakami et al. [148-150], Murakami [59,151,152], Tominaga et al. [145] and others have clearly indicated the deficiencies of steady RANS and the superiority of LES in predicting the extent of separation bubbles and recirculation regions and the magnitude of mean velocity in these regions. However, it might be argued that these regions are less important for PLW, as they are regions with low amplification factors.

7. Best practice guidelines for CFD simulation of pedestrian-level wind speed [1]

The section below provides an overview of best practice guidelines that were either explicitly developed for PLW studies or are of a more general nature but nevertheless applicable to PLW.

In CFD simulations, a large number of choices need to be made by the user. It is well known that these choices can have a very large impact on the results. Already since the start of the application of CFD for wind flow around bluff bodies in the late 70s and 80s, researchers have been testing the influence of these parameters on the results, which has provided a lot of valuable information (e.g. [153-157]). In addition, Schatzmann et al. [158] provided an important contribution on validation with field and laboratory data. However, initially this information was dispersed over a large number of individual publications in different journals, conference proceedings and reports.

In 2000, the ERCOFTAC[2] Special Interest Group on Quality and Trust in Industrial CFD published an extensive set of best practice guidelines for industrial CFD users [128]. These guidelines were focused on RANS simulations. Although they were not specifically intended for wind engineering, many of these guidelines also apply for CFD for PLW. Within the EC project ECORA[3], Menter et al. [159] published best practice guidelines based on the ERCOFTAC guidelines but modified and extended specifically for CFD code validation. Within QNET-CFD[4], the Thematic Area on Civil Construction and HVAC (Heating, Ventilating and Air-Conditioning) and the Thematic Area on the Environment presented some best practice advice for the CFD simulations of wind flow and dispersion [160,161].

---

[1] This section is intentionally and to a large extent reproduced from Blocken [82].

[2] ERCOFTAC = European Research Community on Flow, Turbulence and Combustion

[3] ECORA = Evaluation of Computational Fluid Dynamic Methods for Reactor Safety Analysis

[4] QNET-CFD = Network for Quality and Trust in the Industrial Application of CFD

In 2004, Franke et al. [71] compiled a set of specific recommendations for the use of CFD in wind engineering from a detailed review of the literature, as part of the European COST[5] Action C14: Impact of Wind and Storm on City Life and Built Environment. Later, this contribution was extended into an extensive "Best Practice Guideline for the CFD simulation of flows in the urban environment" [72,73], in the framework of the COST Action 732: Quality Assurance and Improvement of Microscale Meteorological Models, managed by Schatzmann and Britter (http://www.cost.eu/COST_Actions/essem/732). Like the ERCOFTAC guidelines, also these guidelines primarily focused on steady RANS simulations, although also some limited information on URANS, LES and hybrid URANS/LES was provided. When using CFD tools, whether they are academic/open source or commercial codes, it is also important that the code is well documented, and that basic verification tests and validation studies have been successfully performed and reported. A good description of how a microscale airflow and dispersion model has to be documented can be found in the Model Evaluation Guidance Document published in the COST Action 732 by Britter and Schatzmann [162].

In Japan, working groups of the Architectural Institute of Japan (AIJ) conducted extensive cross-comparisons between CFD simulation results and high-quality wind-tunnel measurements to support the development of guidelines for practical CFD applications. Part of these efforts were reported by Yoshie et al. [75]. In 2008, Tominaga et al. [77] published the "AIJ guidelines for practical applications of CFD to pedestrian wind environment around buildings", and Tamura et al. [163] wrote the "AIJ guide for numerical prediction of wind loads on buildings". The guidelines by Tominaga et al. [77] focus on steady RANS simulations, while the guidelines by Tamura et al. [163] also consider LES, given the importance of time-dependent analysis for wind loading of buildings and structures.

As an addition to the valuable guidelines of the COST Actions and the AIJ, Blocken [83] provided ten tips and tricks towards accurate and reliable CFD simulations in urban physics, focused on steady RANS.

More generic best practice advice was provided by Jakeman et al. [164] in the article "Ten iterative steps in development and evaluation of environmental models", which were later on extended to process-based biogeochemical models of estuaries by Robson et al. [165] and to CFD for environmental fluid mechanics (including CWE) by Blocken and Gualtieri [129]. Blocken et al. [70] also provided a general decision framework for the analysis of PLW comfort and safety in urban areas.

The above-mentioned CFD best practice guideline documents have been based on and/or reinforced by more basic guidelines and standards concerning verification and validation, as outlined in e.g. Roache [166,167], AIAA[6] [168], Oberkampf et al. [169], Roy [170], Roy and Oberkampf [171], ASME[7] [172], and others. It is interesting to note that the importance of numerical accuracy control is emphasized by the Journal of Fluids Engineering Editorial Policy [173], incited by contributions by Roache et al. [174] and Freitas [175], which demand at least formally second-order accurate spatial discretization.

In addition to these general guidelines, also some very specific guidelines were published, all of which are very important for CFD for PLW. These include (1) consistent modelling of equilibrium atmospheric boundary layers in computational domains (e.g. [67,72,176-182); (2) high-quality grid generation (e.g. [183,184]) and (3) validation with field and laboratory data (e.g. [158,185]). Note that most of the efforts in the first two areas were focused on steady RANS simulations.

The establishment of these guidelines has been an important step towards more accurate and reliable CFD simulations for PLW. The importance of best practice guidelines in CFD has been stressed by several authors. As an example, a few quotes are given below.

> *"The frequently heard argument 'any solution is better than none' can be dangerous in the extreme. The greatest disaster one can encounter in computation is not instability or lack of convergence but results that are simultaneously good enough to be believable but bad enough to cause trouble." (Ferziger, 1993 [186])*
>
> *"Which model is best for which kind of flows (none is expected to be good for all flows) is not yet quite clear, partly due to the fact that in many attempts to answer this question numerical errors played a too important role so clear conclusions were not possible … In most workshops held so far on the subject of evaluation of turbulence models, the differences between solutions produced by different authors using supposedly the same model were as large if not larger than the differences between the results of the same author using different models." (Ferziger and Peric, 1996 [130])*
>
> *"The very important point, independent of the semantics, is that use of a verified code is not enough. This point is probably well recognized by present readers, but it is not universally so. Especially in the commercial CFD arena, user expectations are often that the purchase and use of a 'really good code' will*

[5] COST = European Cooperation in Science and Technology

[6] AIAA = American Institute of Aeronautics and Astronautics

[7] ASME = American Society of Mechanical Engineers

remove from the user the obligation of 'doing his homework', that is, the straightforward but tedious work of verification of calculations via systematic grid-convergence studies. This unrealistic hope is sometimes encouraged by advertising." (Roache, 1997 [167])

"Most practitioners are more concerned with obtaining results than with either the order of accuracy of their numerical schemes or the need to refine the grid until converged grid-independent solutions are obtained." (Stathopoulos, 1997 [92])

"It is true, of course, that even a highly accurate solution to the modelled equations may differ significantly from the actual flow that would occur given the same boundary conditions, because of inadequacies in the turbulence modelling. But this difference is often of secondary importance compared with those which arise because of 'bad' choices (or even plain user mistakes) in all the other areas." (Castro and Graham, 1999 [187])

"In practice the quality of model output depends not only on the accuracy of the model itself and the model input, but also on the qualification of the person running a model. Numerical simulation is a knowledge-based activity. Appropriate knowledge can be transferred to users by recommendations concerning the proper use of models. For obstacle-resolving CFD codes such recommendations are not straightforward." (Schatzmann and Leitl, 2011 [185])

"The presumption of innocence does not hold in CFD. CFD results are wrong, until proven otherwise" (Blocken, 2014 [82])

8. On the propagation of errors in wind-tunnel and CFD techniques to wind comfort assessment

In the introduction of this paper, it was stated that "the question arises whether 'less accurate' but more inexpensive and faster techniques such as HWA, HFA, Irwin probes, sand erosion and 3D steady RANS CFD simulations can provide sufficiently accurate data on mean wind speed for PLW comfort assessment". In the preceding sections it was repeatedly shown that a large number of previous comparative studies systematically indicate that the low-cost wind-tunnel techniques and steady RANS CFD simulations can provide accurate results (~10%) of mean wind speed in regions of high amplification factors (> 1) while their accuracy can substantially deteriorate in regions of lower amplification factors (< 1). The main hypothesis of this paper is that this does not necessarily compromise the accuracy of PLW comfort assessment, because the higher amplification factors provide the largest contribution to the discomfort exceedance probability in the comfort criterion. To check this hypothesis, in this section we provide a complete wind comfort assessment for a simple case: a high-rise building tower (L x B x H = 40 x 20 x 70 m³) without surrounding buildings on a terrain with aerodynamic roughness length z_0 = 0.25 m. This case was evaluated experimentally by sand erosion tests by Beranek and van Koten [43] and the resulting sand erosion contour plots for different wind directions are shown in Figure 24. We focus on two critical points A and B: for wind direction 0°, point A is situated in the corner stream and point B in the standing vortex. The corner stream and the standing vortex are the areas with the highest amplification factor and represent the most problematic areas for wind comfort. Note however that different wind directions cause the points A and B to be situated in areas of lower amplification factor.

As mentioned in section 1, a wind comfort assessment study should be performed by a combination of three types of information/data: (1) statistical meteorological data; (2) aerodynamic information; and (3) a comfort criterion. Here, we adopt the statistical meteorological data (30 years) of potential wind speed (U_{pot}) at Eindhoven airport. The potential wind speed is the wind speed at 10 m height over a terrain with aerodynamic roughness length z_0 = 0.03 m. Twelve wind directions are considered: 0°, 30°, 60°, …, 330°. The exceedance probability P_θ of U_{pot} in relation to a threshold wind speed $U_{THR,10m}$ at 10 m height can be expressed by a Weibull distribution with parameters a, c and k fitted based on the statistical meteorological data:

$$P_\theta = P_\theta\left(U_{pot} > U_{THR,10m}\right) = 100 \cdot A(\theta(\cdot \exp\left[-\left(\frac{U_{THR,10m}}{c(\theta)}\right)^{k(\theta)}\right] \quad (14)$$

For simplicity, in this section we assume that every wind direction has the same frequency occurrence and the same contribution to the wind statistics, and that the exceedance probability for a given threshold value for every wind direction is 1/12th of the sum of the exceedance probabilities for all wind directions:

$$P_\theta' = P_\theta'(U_{pot} > U_{THR,10m}) = \frac{100}{12} \cdot \sum_{\theta=0°}^{330°} \left[A(\theta(\cdot \exp\left[-\left(\frac{U_{THR,10m}}{c(\theta)} \right)^{k(\theta)} \right] \right] \quad (15)$$

The aerodynamic information can be decomposed in a terrain-related contribution (U_0/U_{pot}) and a design-related contribution ($K = U/U_0$) with U_0 the local reference wind speed, i.e. the wind speed at the building site at 1.75 m (pedestrian height) without buildings present (see Fig. 1). The design-related contribution is given by the local amplification factor K in Figure 24. The terrain-related contribution is obtained by combining the expression of the vertical mean wind speed profile by the logarithmic law and the wind speed conversion using the blending height of 60 m [14]. The comfort criterion is the one by the Dutch Standard NEN 8100, with threshold wind speed U_{THR} = 5 m/s and exceedance probabilities linked to different activities and quality classes (Table 1). However, also other threshold wind speed values will be considered in this section.

Figure 25a expresses the total exceedance probability $P = \Sigma 12 P_\theta$' as a function of the local amplification factor K with U_{THR} as a parameter. It indicates to which extent amplification factor values contribute to the total exceedance probability. It clearly shows that larger value of K contribute more to the exceedance probability but that this is also governed by the choice of U_{THR}. Figure 25b shows the derivative of P to K with U_{THR} as parameter. It indicates the sensitivity of P to changes in K and hence the extent to which errors in K will propagate to errors in P.

As an illustration of the extent to which errors in K (either by wind-tunnel testing or by CFD) in a realistic case of PLW assessment propagate to errors in P, two different sets of K values are considered. The first set corresponds to the values in Figure 24. The second set is created from the first set by changes taking into account the error levels in Table 4. This yields the values of modified K (K_{mod}) in Table 5. The magnitude of the error levels is chosen based on Figure 22a but assuming to some extent a worst-case scenario, i.e. all errors are underestimations, so there is no compensation of underestimations by overestimations as can be the case in reality as shown in Figure 22a. Application of the total wind comfort procedure consists of combining Table 5 and Figure 25a, which yields Figure 26. The numerical values of the differences (i.e. errors) are given in Table 6. The following observations are made:

- For all values of U_{THR}: In spite of the large errors imposed on especially the lower amplification factors, the errors in P remain fairly limited. It should be noted that in reality it is likely that errors due to overestimations and underestimations of K will compensate each other, and the total errors in P can be smaller than those in the present study.
- The differences in Figure 26 and Table 6 are largest for U_{THR} = 3 m/s and smallest for U_{THR} = 8 and 10 m/s. This is a direct result of the range of amplification factors considered (see Table 5) and of the sensitivity dP/dK shown in Figure 25b. As a result, it is clear that the choice of the comfort criterion can actually co-determine the accuracy of the wind comfort assessment results.
- While one can argue that the amplification factor errors will be larger in points other than A and B in less windy regions where the amplification factors are lower , it should be noted that the points with the highest amplification factors are generally of most interest as these represent the most important positions from the viewpoint of wind comfort.

9. Discussion

9.1. Limitations of this paper

This paper has reviewed different wind-tunnel techniques for the measurement of PLW speed. It has also reviewed previous comparison studies that provide some information on the relative accuracy of the different techniques. Also best practice guidelines for wind-tunnel measurement of PLW have been briefly highlighted. The paper has also reviewed CFD techniques for PLW studies, as well as previous studies comparing RANS CFD simulations with wind-tunnel measurements and on-site measurements, with also some comments on non-PLW studies comparing LES and RANS. Also many of the important best practice guidelines for the CFD simulation of PLW speed have been highlighted. A main limitation of these reviews is that they have almost exclusively focused on measuring or simulating mean wind speed, rather than an effective wind speed that includes gustiness to some degree. It is widely acknowledged that gustiness is important for wind comfort. Nevertheless, many comfort criteria (e.g. 3 out of the four in Table 3) do not explicitly include gustiness. It is believed that they include gustiness implicitly, by a raised value of the mean wind speed threshold U_{THR}. Future studies can include comparative studies focused on measuring and simulating gustiness.

In section 8, the paper has presented a small and exemplary wind comfort assessment study to illustrate the way in which errors in wind-tunnel or CFD estimates of mean wind speed propagate to errors in the exceedance probability P that is the final result of the wind comfort assessment procedure. It was shown that the error

propagation is limited because the errors are largest for the lower amplification factors which are also those that generally contribute the least to the discomfort exceedance probability. The exercise in section 8 has its limitations. It is only one example to illustrate that errors in wind-tunnel measurement or CFD simulation of mean wind speed at low amplification factors do not necessarily compromise the accuracy of PLW comfort assessment. This exercise only considered the wind speed statistics of the Eindhoven airport meteorological station and only a single high-rise building in an area with $z_0 = 0.25$ m. The exercise can now easily be repeated for different sets of statistical meteorological data and different building configurations.

The extent of error propagation is determined by a wide range of factors: the wind statistics at the location of interest, the building configuration, the points around the building(s) in which wind speed is evaluated, and even the wind speed threshold value in the comfort criterion. Future research might therefore consider applying different wind speed threshold values as to maximize the accuracy of the PLW comfort assessment procedure.

9.2. Wind-tunnel versus RANS and LES

For decades, the atmospheric boundary layer wind tunnel has been the standard tool to determine the design-related contribution in PLW studies. In the past 15 years, CFD has entered the scene. In the past decade, several researchers have adequately highlighted possibilities and limitations of CFD in general and of RANS and LES in particular. Stathopoulos [6,93] states that, in spite of many difficulties of CFD applications, there have been cases for which the application of CFD appears to give somewhat satisfactory responses, such as those focused on the determination of mean flow conditions and pressures, i.e. those related primarily with environmental issues. Examples are PLW, snow dispersion and accumulation, pollutant dispersion and ventilation [6]. In particular, he correctly argues that PLW can be described quite adequately in terms of mean velocities in the presence and absence of a new building within a specific urban environment [6]. While pedestrians are mostly affected by gust effects and mean wind speeds may not be sufficient to produce satisfactory results, Stathopoulos [6] stresses that the fact remains that several major cities require only the satisfaction of certain mean (sustainable) speeds with a specified probability of exceedance.

It is generally acknowledged that RANS CFD is deficient in reproducing turbulence intensities and gustiness and that LES has the intrinsic ability to provide accurate estimates of these variables. However, if the PLW study remains focused on mean wind speed rather than on an effective wind speed, RANS CFD simulations could be sufficient. This in itself might be a reason to limit PLW studies to mean wind speed and to focus on wind comfort and wind safety criteria only considering mean wind speed, although it is clear that this approach entails limitations. Gusts are important for wind comfort and wind safety, and criteria only considering mean wind speed generally already include an artificial increase in the threshold mean wind speed value to take into account gustiness issues.

It is expected that for particular applications, when accurate reproduction of large-scale turbulent structures and the related heat and mass transport are important, e.g. in pollutant dispersion studies [188-190], LES will increasingly replace RANS. This expectation is even more pronounced where wind loading is concerned. For PLW on the other hand, where information about mean wind velocity fields could be sufficient, it is not clear at all whether LES will replace RANS. In this perspective, Hanjalic [191] stated in 2004 that RANS will continue to play an important role, especially in industrial and environmental computations, and that the further increase in the computing power will be used more to utilize advanced RANS models to shorten the design and marketing cycle rather than to yield the way to LES.. In 2007, Baker [192] anticipated that CFD applications will become widespread in areas where wind velocities rather than surface pressures are required, such as the assessment of pedestrian comfort, which may well lead to the concentration of boundary layer wind tunnel testing for complex structures into a smaller number of institutions over the next few decades [192]. He also mentioned that the use of RANS based techniques will decrease over time, although their relative simplicity and economy will ensure their continued use for many applications [192].

9.3. Uncertainty quantification

Wind-tunnel measurements and CFD simulations have in common that they are only capable of representing part of the complexity of the actual problem under study. Typical examples are the assumption of neutral atmospheric boundary layer flow, which is common in both wind-tunnel testing and CFD, the assumption of a uniformly rough upstream fetch with a given roughness length, the assumption of a given sand-grain roughness for street and building surfaces, etc. Uncertainty quantification refers to the group of actions devoted to the quantitative characterization and reduction of uncertainties in wind-tunnel testing and CFD simulations. These actions are important to assess the actual predictive capabilities of these methodologies. A distinction can be made between two types of uncertainties: aleatory uncertainty and epistemic uncertainty. Aleatory uncertainty refers to the uncertainty due to the physical variability of the system and is inherent to the modeled system. Epistemic uncertainty is the uncertainty due to a lack of knowledge [193].

In the field of wind engineering in general and in the study of PLW in particular, many past efforts have implicitly performed a certain degree of uncertainty quantification. Typical examples are the majority of comparative wind-tunnel studies and CFD studies cited in this paper. A more explicit and systematic focus on uncertainty quantification for wind engineering flow has been adopted by e.g. Garcia-Sanchez et al. [194] and Gorlé et al. [195].

Epistemic uncertainty can be limited by more accurate wind-tunnel measurement techniques and more accurate CFD models, e.g. LES versus RANS. However, the high degree of aleatory uncertainty in urban aerodynamics including PLW, implies that reducing the epistemic uncertainty will not necessarily yield a large improvement of the predictive capabilities of the measurements or simulations. This very fact could indeed be seen as additional support for the main message of the present paper: being that "less accurate" but less expensive and faster techniques such as HWA, HFA, Irwin probes, sand erosion and 3D steady RANS CFD simulations can provide sufficiently accurate data on mean wind speed for PLW comfort assessment.

10. Conclusions

Information on pedestrian-level wind (PLW) speed for wind comfort assessment can be obtained with wind-tunnel measurements or Computational Fluid Dynamics (CFD). Wind-tunnel measurements for PLW are routinely performed with low-cost techniques such as hot-wire or hot-film anemometers (HWA or HFA), Irwin probes or sand erosion, while Laser-Doppler Anemometry (LDA) and Particle-Image Velocimetry (PIV) are less often used because they are more expensive. CFD simulations are routinely performed by the relatively low-cost steady Reynolds-Averaged Navier-Stokes (RANS) approach. Large-Eddy Simulation (LES) is less often used because of its larger complexity and cost.

The question arises whether "less accurate" but more inexpensive and faster techniques such as HWA, HFA, Irwin probes, sand erosion and 3D steady RANS CFD simulations can provide sufficiently accurate data on mean wind speed for PLW comfort assessment. If so, this would justify the vast majority of past research efforts and support the continued use of these low-cost and relatively fast techniques for this type of studies. If not, this would motivate the transition to more expensive techniques such as LDA, PIV and LES. This paper has attempted to answer this question.

Indeed, this paper has reviewed different wind-tunnel and CFD techniques to determine PLW speed, with a specific focus on their advantages and disadvantages. Next, this paper has reviewed some comparative studies that systematically indicate that the low-cost wind-tunnel techniques and steady RANS simulations can provide accurate results (~10%) in areas of high amplification factors (> 1) while their accuracy can deteriorate in areas of lower amplification factors (< 1). Because high amplification factors contribute most to the discomfort threshold exceedance probability in the wind comfort criterion, the hypothesis was stated that the smaller accuracy in areas of lower amplification factors does not necessarily compromise the accuracy of the overall wind comfort assessment. An example wind comfort assessment study has shown that this is indeed the case. As a result, although LDA, PIV and LES are inherently more accurate techniques, this paper supports the continued use of faster and less expensive techniques for PLW studies. Extrapolating the words of the late professor Ferziger [196], we conclude that *pedestrian-level wind comfort is one of the few topics in wind engineering where nature is kind to us concerning turbulent flows.*

Acknowledgments

This paper is dedicated to the memory of the late Prof. dr. Alan G. Davenport and the late Prof. dr. Joel H. Ferziger. Professor Alan G. Davenport (September 19, 1932 – July 19, 2009) was a Wind Engineering professor at the University of Western Ontario (UWO), London, Canada and founder of the Boundary Layer Wind Tunnel Laboratory at UWO. The second author of this paper was very fortunate to obtain his graduate degrees working under his inspiring supervision. Professor Ferziger (24 March 1937 – 16 August 2004) was a professor of Fluid Mechanics at the Thermosciences Division at Department of Mechanical Engineering at Stanford University, USA. His over-inspiring lectures and publications have been always characterized by simplicity, boldness and humbleness. This paper is dedicated to them because of their pioneering contributions to experimental and computational wind engineering, including the assessment of pedestrian-level wind comfort and wind safety, which undoubtedly have improved comfort and have saved lives in cities all over the world.

References

[1] Wise AFE. 1970. Wind effects due to groups of buildings, Proceedings of the Royal Society Symposium Architectural Aerodynamics, Session 3, Effect of Buildings on the Local wind, London. pp. 26–27 February.

[2] Lawson TV, Penwarden AD. 1975. The effects of wind on people in the vicinity of buildings, Proceedings 4th International Conference on Wind Effects on Buildings and Structures, Cambridge University Press, Heathrow, pp. 605–622.
[3] Soligo MJ, Irwin PA, Williams CJ, Schuyler GD. 1998. A comprehensive assessment of pedestrian comfort including thermal effects. J Wind Eng Ind Aerodyn 77–78: 753-766.
[4] ASCE, 1999. ASCE Wind tunnel studies of buildings and structures. Aerospace Division of the American Society of Civil Engineers. ISBN (print): 978-0-7844-0319-8.
[5] ASCE, 2004. Outdoor human comfort and its assessment: state of the art. American Society of Civil Engineers Task Committee on Outdoor Human Comfort of the Aerodynamics Committee, Reston, VA.
[6] Stathopoulos T. 2006. Pedestrian level winds and outdoor human comfort. J Wind Eng Ind Aerodyn 94(11): 769-780.
[7] Metje N, Sterling M, Baker CJ. 2008. Pedestrian comfort using clothing values and body temperatures. J Wind Eng Ind Aerodyn 96(4): 412-435.
[8] van Hooff T, Blocken B, van Harten M. 2011. 3D CFD simulations of wind flow and wind-driven rain shelter in sports stadia: influence of stadium geometry. Build Environ 46(1): 22-37.
[9] van Hooff T, Blocken B. 2012. Full-scale measurements of indoor environmental conditions and natural ventilation in a large semi-enclosed stadium: possibilities and limitations for CFD validation. J Wind Eng Ind Aerodyn 104-106: 330-341.
[10] van Hooff T, Blocken B. 2013. CFD evaluation of natural ventilation of indoor environments by the concentration decay method: CO_2 gas dispersion from a semi-enclosed stadium. Build Environ 61:1-17
[11] Willemsen E, Wisse JA. 2007. Design for wind comfort in The Netherlands: Procedures, criteria and open research issues. J Wind Eng Ind Aerodyn 95(9-11): 1541-1550.
[12] Wieringa J. 1992. Updating the Davenport roughness classification. J Wind Eng Ind Aerodyn 41-44, 357-368.
[13] Simiu E, Scanlan RH. 1986. Wind effects on structures. An introduction to wind engineering, Second Ed. Wiley, New York.
[14] Verkaik JW. 2006. On wind and roughness over land. PhD thesis. Wageningen University. The Netherlands, 123 p.
[15] NEN 2006. Application of mean hourly wind speed statistics for the Netherlands, NPR 6097:2006 (in Dutch). Dutch Practice Guideline.
[16] Bottema M. 2000. A method for optimisation of wind discomfort criteria. Build Environ 35(1), 1-18.
[17] Koss HH. 2006. On differences and similarities of applied wind comfort criteria. J Wind Eng Ind Aerodyn 94: 781-797.
[18] Janssen WD, Blocken B, van Hooff T. 2013. Pedestrian wind comfort around buildings: comparison of wind comfort criteria based on whole-flow field data for a complex case study. Build. Environ. 59: 547-562.
[19] NEN 2006. Wind comfort and wind danger in the built environment, NEN 8100 (in Dutch) Dutch Standard.
[20] Isyumov N, Davenport AG. 1975. The ground level wind environment in built-up areas. In: Proceedings of Fourth International Conference on Wind Effects on Buildings and Structures. Heathrow, UK, Cambridge University Press, 403-422.
[21] Lawson TV. 1978. The wind content of the built environment. J Ind Aerodyn 3:93-105.
[22] Melbourne WH. 1978. Criteria for environmental wind conditions. J Ind Aerodyn 3:241-249.
[23] Isyumov N, Davenport AG. 1975. Comparison of full-scale and wind tunnel wind speed measurements in the commerce court plaza. J Wind Eng Ind Aerodyn 1: 201-212
[24] Kamei I, Maruta E. 1979. Study on wind environmental problems caused around buildings in Japan. J Wind Eng Ind Aerodyn 4(3–4): 307-331.
[25] Stathopoulos T. 1985. Wind environmental conditions around tall buildings with chamfered corners. J Wind Eng Ind Aerodyn 21(1): 71-87.
[26] Stathopoulos T, Storms R. 1986. Wind environmental conditions in passages between buildings. J Wind Eng Ind Aerodyn 24(1): 19-31.
[27] Kawamura S, Kimoto E, Fukushima T, Tanike Y. 1988. Environmental wind characteristics around the base of a tall building - A comparison between model test and full-scale experiment. J Wind Eng Ind Aerodyn 28: 149-158.
[28] Ratcliff MA, Peterka JA. 1990. Comparison of pedestrian level wind acceptability criteria. J Wind Eng Ind Aerodyn 36:791-800.
[29] Lam KM. 1992. Wind environment around the base of a tall building with a permeable intermediate floor. J Wind Eng Ind Aerodyn. 44(1–3): 2313-2314.

[30] Uematsu Y, Yamada M, Higashiyama H, Orimo T. 1992. Effects of the corner shape of high-rise buildings on the pedestrian-level wind environment with consideration for mean and fluctuating wind speeds. J Wind Eng Ind Aerodyn 44(1–3): 2289-2300.
[31] Jamieson NJ, Carpenter P, Cenek PD. 1992. The effect of architectural detailing on pedestrian level wind speeds. J Wind Eng Ind Aerodyn. 44(1–3): 2301-2312.
[32] Blocken B, Stathopoulos T, Carmeliet J. 2008a. Wind environmental conditions in passages between two long narrow perpendicular buildings. Journal of Aerospace Engineering - ASCE. 21(4): 280-287.
[33] Blocken B, Moonen P, Stathopoulos T, Carmeliet J. 2008b. A numerical study on the existence of the Venturi-effect in passages between perpendicular buildings. J Eng Mech-ASCE 134(12): 1021-1028.
[34] Bradbury LJS, Castro, IP. 1971. A pulsed wire technique for velocity measurements in highly turbulent flows. J Fluid Mech 49: 657.
[35] Britter RE, Hunt JCR. 1979. Velocity measurements and order of magnitude estimates of the flow between two buildings in a simulated atmospheric boundary layer. J Wind Eng Ind Aerodyn 4(2): 165-182.
[36] Castro IP. 1992. Pulsed-wire anemometry. Experimental Thermal and Fluid Science 5: 770-780.
[37] Irwin HPAH. 1981. A simple omnidirectional sensor for wind-tunnel studies of pedestrian-level winds. J Wind Eng Ind Aerodyn. 7(3): 219-239.
[38] Durgin FH. 1992. Pedestrian level wind studies at the Wright brothers facility. J Wind Eng Ind Aerodyn. 44(1–3): 2253-2264.
[39] Wu H, Stathopoulos T. 1994. Further experiments on Irwin's surface wind sensor. J Wind Eng Ind Aerodyn 53(3): 441-452.
[40] Monteiro JP, Viegas DX. 1996. On the use of Irwin and Preston wall shear stress probes in turbulent incompressible flows with pressure gradients. J Wind Eng Ind Aerodyn 64(1): 15-29.
[41] Van Beeck JPAJ, Dezsö G, Planquart P. 2009. Microclimate assessment by sand erosion and Irwin probes for atmospheric boundary layer wind tunnels. PHYSMOD 2009, Von Karman Institute (VKI), Sint-Genesius-Rode, Belgium.
[42] Tsang CW, Kwok KCS, Hitchcock PA. 2012. Wind tunnel study of pedestrian level wind environment around tall buildings: Effects of building dimensions, separation and podium. Build Environ 49: 167-181.
[43] Beranek WJ, van Koten H. 1979a. Visual techniques for the determination of wind environment. J Wind Eng Ind Aerodyn 4(3–4): 295-306.
[44] Beranek WJ, van Koten H. 1979b. Beperken van windhinder om gebouwen, deel 1, Stichting Bouwresearch no. 65, Kluwer Technische Boeken BV, Deventer (in Dutch).
[45] Beranek WJ. 1982. Beperken van windhinder om gebouwen, deel 2, Stichting Bouwresearch no. 90, Kluwer Technische Boeken BV, Deventer (in Dutch).
[46] Livesey F, Inculet D, Isyumov N, Davenport AG. 1990. A scour technique for the evaluation of pedestrian winds. J Wind Eng Ind Aerodyn 36(2): 779-789.
[47] Livesey F, Morrish D, Mikitiuk M, Isyumov N. 1992. Enhanced scour tests to evaluate pedestrian level winds. J Wind Eng Ind Aerodyn 44(1–3): 2265-2276.
[48] Richards PJ, Mallison GD, McMillan D, Li YF. 2002. Pedestrian level wind speeds in downtown Auckland. Wind Struct 5(2–4): 151–164.
[49] Conan B, van Beeck J, Aubrun S. 2012. Sand erosion technique applied to wind resource assessment. J Wind Eng Ind Aerodyn 104–106: 322-329.
[50] Yamada M, Uematsu Y, Sasaki R. 1996. A visual technique for the evaluation of the pedestrian-level wind environment around buildings by using infrared thermography. J Wind Eng Ind Aerodyn 65(1–3): 261-271.
[51] Wu H, Stathopoulos T. 1997. Application of infrared thermography for pedestrian wind evaluation. J Eng Mech–ASCE 123(10): 978–985
[52] Sasaki R, Uematsu Y, Yamada M, Saeki H. 1997. Application of infrared thermography and a knowledge-based system to the evaluation of the pedestrian-level wind environment around buildings. J Wind Eng Ind Aerodyn 67–68: 873-883.
[53] Murakami, S., 1990. Computational wind engineering. J. Wind Eng. Ind. Aerodyn. 36 (1), 517–538.
[54] Gadilhe A, Janvier L, Barnaud G. 1993. Numerical and experimental modelling of the three-dimensional turbulent wind flow through an urban square. J Wind Eng Ind Aerodyn 46-47: 755-763.
[55] Takakura S, Suyama Y, Aoyama M. 1993. Numerical simulation of flowfield around buildings in an urban area. J Wind Eng Ind Aerodyn 46-47: 765-771.
[56] Bottema M. 1993. Wind climate and urban geometry, PhD thesis, Eindhoven University of Technology.
[57] Stathopoulos T, Baskaran A. 1996. Computer simulation of wind environmental conditions around buildings. Eng Struct 18(11): 876–885.
[58] Baskaran, A., Kashef, A. 1996. Investigation of air flow around buildings using computational fluid dynamics techniques. Engineering Structures 18 (11), 861-873.

[59] Murakami, S. 1997. Current status and future trends in computational wind engineering. Journal of Wind Engineering and Industrial Aerodynamics 67 & 68: 3-34.
[60] Ferreira AD, Sousa ACM, Viegas DX. 2002. Prediction of building interference effects on pedestrian level comfort. J Wind Eng Ind Aerodyn 90: 305–319.
[61] Mochida, A.,Tominaga,Y.,Murakami,S.,Yoshie,R.,Ishihara,T.,Ooka,R., 2002. Comparison of various k-ε models and DSM applied to flow around a high-rise building—report on AI Jcooperative project for CFD prediction of wind environment. Wind Struct. 5(2–4), 227–244.
[62] Meroney RN, Neff DE, Chang CH, Predoto R. 2002. Computational Fluid Dynamics and physical model comparisons of wind loads and pedestrian comfort around a high rise building, Session on Computational Evaluation of Wind Effects on Buildings, Proceedings of ASCE 2002 Structures Congress, Denver, CO, April 4-6, 2002, 2 pp.
[63] Miles SD, Westbury PS. 2002. Assessing CFD as a tool for practical wind engineering applications. In: Proceedings of the Fifth UK Conference on Wind Engineering, September.
[64] Westbury PS, Miles SD, Stathopoulos T. 2002. CFD application on the evaluation of pedestrian-level winds. In: Proceedings of the Workshop on Impact of Wind and Storm on City Life and Built Environment, Cost Action C14, CSTB, June 3–4, Nantes, France.
[65] Hirsch C, Bouffioux V, Wilquem F. 2002. CFD simulation of the impact of new buildings on wind comfort in an urban area. Workshop Proceedings, Cost Action C14, Impact of Wind and Storm on City Life and Built Environment, Nantes, France.
[66] Blocken B, Roels S, Carmeliet J. 2004. Modification of pedestrian wind comfort in the Silvertop Tower passages by an automatic control system. J Wind Eng Ind Aerodyn 92 (10): 849-873.
[67] Blocken B, Carmeliet J, Stathopoulos T. 2007a. CFD evaluation of the wind speed conditions in passages between buildings – effect of wall-function roughness modifications on the atmospheric boundary layer flow. J Wind Eng Ind Aerodyn 95(9-11): 941-962.
[68] Blocken B, Carmeliet J. 2008. Pedestrian wind conditions at outdoor platforms in a high-rise apartment building: generic sub-configuration validation, wind comfort assessment and uncertainty issues. Wind Struct 11(1): 51-70.
[69] Blocken B, Persoon J. 2009. Pedestrian wind comfort around a large football stadium in an urban environment: CFD simulation, validation and application of the new Dutch wind nuisance standard. J Wind Eng Ind Aerodyn 97(5-6): 255-270.
[70] Blocken B, Janssen WD, van Hooff T. 2012. CFD simulation for pedestrian wind comfort and wind safety in urban areas: General decision framework and case study for the Eindhoven University campus. Environ Modell Softw 30: 15-34.
[71] Franke J, Hirsch C, Jensen AG, Krüs HW, Schatzmann M, Westbury PS, Miles SD, Wisse JA, Wright NG. 2004. Recommendations on the use of CFD in wind engineering. Proc. Int. Conf. Urban Wind Engineering and Building Aerodynamics, (Ed. van Beeck JPAJ), COST Action C14, Impact of Wind and Storm on City Life Built Environment, von Karman Institute, Sint-Genesius-Rode, Belgium, 5 - 7 May 2004
[72] Franke J, Hellsten A, Schlünzen H, Carissimo B. 2007. Best practice guideline for the CFD simulation of flows in the urban environment. COST 732: Quality Assurance and Improvement of Microscale Meteorological Models.
[73] Franke J, Hellsten A, Schlünzen H, Carissimo B. 2011. The COST 732 best practice guideline for CFD simulation of flows in the urban environment – A summary. Int J Environ Pollut 44(1-4): 419-427.
[74] Zhang A, Gao C, Zhang L. 2005. Numerical simulation of the wind field around different building arrangements. J Wind Eng Ind Aerodyn 93(12): 891-904.
[75] Yoshie R, Mochida A, Tominaga Y, Kataoka H, Harimoto K, Nozu T, Shirasawa T. 2007. Cooperative project for CFD prediction of pedestrian wind environment in the Architectural Institute of Japan. J Wind Eng Ind Aerodyn 95(9-11): 1551-1578.
[76] Mochida A, Lun IYF. 2008. Pedestrian wind environment and thermal comfort at pedestrian level in urban area. J Wind Eng Ind Aerodyn 96: 1498-1527.
[77] Tominaga Y, Mochida A, Yoshie R, Kataoka H, Nozu T, Yoshikawa M, Shirasawa T. 2008a. AIJ guidelines for practical applications of CFD to pedestrian wind environment around buildings. J Wind Eng Ind Aerodyn 96(10-11): 1749-1761.
[78] Bady M, Kato S, Ishida Y, Huang H, Takahashi T. 2011. Application of exceedance probability based on wind kinetic energy to evaluate the pedestrian level wind in dense urban areas. Building and Environment 46(9): 1834-1842.
[79] Moonen P, Defraeye T, Dorer V, Blocken B, Carmeliet J. 2012. Urban physics: effect of the microclimate on comfort, health and energy demand. Frontiers of Architectural Research 1(3): 197-228.

[80] Montazeri H, Blocken B, Janssen WD, van Hooff T. 2013. CFD evaluation of new second-skin facade concept for wind comfort on building balconies: Case study for the Park Tower in Antwerp. Build Environ 68: 179-192.
[81] Meroney RN, Derickson R. 2014. Virtual reality in wind engineering: the windy world within the computer. Journal of Wind Engineering 11(2): 11-26.
[82] Blocken B. 2014. 50 years of Computational Wind Engineering: Past, present and future. J Wind Eng Ind Aerodyn 129: 69-102.
[83] Blocken B. 2015. Computational Fluid Dynamics for Urban Physics: Importance, scales, possibilities, limitations and ten tips and tricks towards accurate and reliable simulations. Build Environ 91: 219-245.
[84] Shi X, Zhu Y, Duan J, Shao R, Wang J. 2015. Assessment of pedestrian wind environment in urban planning design. Landscape and Urban Planning 140: 17-28.
[85] Vernay DG, Raphael B, Smith IFC. 2015. Improving simulation predictions of wind around buildings using measurements through system identification techniques. Build Environ 94(2): 620-631.
[86] He J, Song CCS. 1999. Evaluation of pedestrian winds in urban area by numerical approach. J Wind Eng Ind Aerodyn 81: 295–309.
[87] Razak AA, Hagishima A, Ikegaya N, Tanimoto J. 2013. Analysis of airflow over building arrays for assessment of urban wind environment. Build Environ 59: 56-65.
[88] Ettounney SM, Fricke FR. 1975. An anemometer for scale model environmental wind measurements. Building Science 10(1): 17-26.
[89] Irwin HPAH. 1982. Instrumentation considerations for velocity measurements. Proc. Int. Worshop on Wind Tunnel Modelling Criteria and Techniques in Civil Engineering Application. Reinhold T.A., Ed., Cambridge University Press, New York, 546-557.
[90] Beranek WJ. 1984. Wind environment around building configurations, Heron, 29(1): 33–70.
[91] Wu H, Stathopoulos T. 1993. Wind-tunnel techniques for assessment of pedestrian-level winds. Journal of Engineering Mechanics 119(10): 1920-1936.
[92] Stathopoulos, T. 1997. Computational Wind Engineering: Past achievements and future challenges. J. Wind Eng. Ind. Aerodyn. 67-68: 509-532.
[93] Stathopoulos T. 2002. The numerical wind tunnel for industrial aerodynamics: real or virtual in the new millennium? Wind Struct. 5(2–4): 193–208.
[94] Blocken, B., Stathopoulos T, Carmeliet, J., Hensen, J.L.M., 2011. Application of CFD in building performance simulation for the outdoor environment: an overview. J. Building Perform. Simul. 4(2), 157-184.
[95] Blocken B, Stathopoulos T. 2013. Editorial to virtual special issue: CFD simulation of pedestrian-level wind conditions around buildings: past achievements and prospects. J Wind Eng Ind Aerodyn 121: 138-145.
[96] Plate EJ. 1982. Engineering meteorology: fundamentals of meteorology and their application to problems in environmental and civil *engineering*. Elsevier Scientific Publishing, 740 pp.
[97] Simiu E, Scanlan RH .1996. Wind effect on structures. Fundamentals and applications to design. Third Edition. Ed. Wiley-Interscience, 704 p.
[98] Penwarden AD, Wise AFE. 1975. Wind environment around buildings, Building Research Establishment Report, Department of Environment, BRE, HMSO, London, UK.
[99] Wiren BG. 1975. A wind tunnel study of wind velocities in passages between and through buildings, In: Proceedings of the 4th International Conference on Wind Effects on Buildings and Structures, Cambridge University Press, Heathrow, pp. 465–475.
[100] Murakami S, Uehara K, Komine H. 1979. Amplification of wind speed at ground level due to construction of high-rise building in urban area. J Wind Eng Ind Aerodyn 4(3–4): 343-370.
[101] White BR. 1992. Analysis and wind tunnel simulation of pedestrian-level winds in San Francisco. J Wind Eng Ind Aerodyn 44(1–3): 2353-2364.
[102] Isyumov N. 1978. Studies of the pedestrian level wind environment at the boundary layer wind tunnel laboratory of the University of Western Ontario. J Wind Eng Ind Aerodyn 3(2–3): 187-200.
[103] Handford PM, Bradshaw P. 1989. The pulsed hot wire anemometer, Exp Fluids 7, 125-132, 1989
[104] Castro IP, Cheun BS. 1982. The measurement of Reynolds stresses with a pulsed wire anemometer. Journal of Fluid Mechanics 118: 41-58.
[105] Castro IP, Diana M. 1990. Pulsed wire anemometry near walls. Experiments in Fluids 8: 343-352.
[106] Williams CD, Wardlaw RL. 1992. Determination of the pedestrian wind environment in the city of Ottawa using wind tunnel and field measurements. J Wind Eng Ind Aerodyn 41(1–3): 255-266.
[107] Dezsö G. 2006. On assessment of wind comfort by sand erosion. PhD thesis. Eindhoven University of Technology, The Netherlands. ISBN:2-930389-22-2.
[108] Bradshaw, P., Huang, G., 1995. The law of the wall in turbulent flow. Proceedings of the Royal Society of London A 451 (1941), 165.

[109] Cheung T. 1977. Evaluation of ground level wind environment for simple buildings and groupings. Faculty of Engineering Science, The University of Western Ontario, ES 400 Report.
[110] Borges ARJ, Saraiva JAG. 1979. An erosion technique for assessing ground level winds. In: Proceedings of the 5th International Conference on Wind Engineering, Fort Collins, Colorado State University, Colorado, Part 1, pp. 235–242.
[111] Isyumov et al. 1986. A study of the pedestrian level winds for the Canary Wharf Project, London, England. Engineering Science Research Report, BLWT-SS16-1986.
[112] Isyumov N, Amos K. 1986. An investigation of pedestrian level wind and snow drifting patterns for the Cityfront Plaza, Chicago, Illinois, USA. Engineering Science Research Report, B LWT-SS33-1986.
[113] Surry D, Georgiou PN. An investigation of wind effects for the Prudential Property Project, Irvine, California, USA. Engineering Science Research Report, BLWT-SS16-1988.
[114] Yamada M., Uematsu Y., Koshihara T., J. Wind Eng. JAWE 35 (1988a) 35 (in Japanese with English summary).
[115] Yamada M., Uematsu Y., Koshihara T., J. Wind Eng. JAWE 36 (1988b) 1 (in Japanese with English summary).
[116] Uematsu Y., Yamada M., Kikuchi M., J. Wind Eng. JAWE 43 (1990) 9 (in Japanese with English summary).
[117] Winter 1976. An outline of the techniques available for the measurement of skin friction in turbulent boundary layers, Prog. Aerospace Sci., 18, 1-57 (1977), also VKI LS 86, March 1976, von Karman Institute.
[118] Grässer A, Hühnergarth A, Schnotale D. 1990. Non-rotating instrument for simultaneous measurement of wind velocity and wind direction. Technisches Messen, Münich, Germany 57(12): 469-472.
[119] Olsen E, Strindehag 0. 1991. An investigation of a sonic flowmeter. J Wind Eng Ind Aerodyn 37: 245-253.
[120] Snyder WH. 1981. Guideline for fluid modeling of atmospheric diffusion. Rep. No. EPA-600/8-81-009, U.S. Environmental Protection Agency, Washington, D.C.
[121] von Karman Th. 1930. Mechanische Ähnlichkeit und Turbulenz, Nachrichten von der Gesellschaft der Wissenchaften zu Göttingen, Fachgruppe 1 (Mathematik) **5**: 58–76 (also as: “Mechanical Similitude and Turbulence”, Tech. Mem. NACA, no. 611, 1931).
[122] Dezső G, Massini M, van Beeck JPAJ. 2003. Pedestrian wind comfort approached by PIV and sand erosion, PHYSMOD2003 - International Workshop on Physical Modelling of Flow and Dispersion Phenomena, Prato, Italy, September 3-5, 2003.
[123] Visser GT, Cleijne JW. 1994. Wind comfort predictions by wind tunnel tests: comparison with full-scale data. J Wind Eng Ind Aerodyn 52: 385-402
[124] Dye RCF. 1980. Comparison of full-scale and wind-tunnel model measurements of ground winds around a tower building, J Wind Eng Ind Aerodyn 6: 311-326.
[125] Gandemer J., Simulation and measurement of the local wind environment, Proc. Workshop Wind Tunnel Modelling for Civil Engineering Applications, Gaithersburg, USA, April 1982.
[126] Sanz Rodrigo J, van Beeck J, Buchlin JM. 2012. Wind engineering in the integrated design of princess Elisabeth Antartic base. Build Environ 52: 1-18.
[127] Cochran LS, Howell JF. 1990. Wind tunnel studies for the aerodynamic shape of Sydney, Australia. J Wind Eng Ind Aerodyn 36: 801-810.
[128] Casey M, Wintergerste T. 2000. Best Practice Guidelines, ERCOFTAC Special Interest Group on Quality and Trust in Industrial CFD, ERCOFTAC, Brussels.
[129] Blocken B, Gualtieri C. 2012. Ten iterative steps for model development and evaluation applied to Computational Fluid Dynamics for Environmental Fluid Mechanics. Environ Modell Softw 33: 1-22.
[130] Ferziger JH, Peric M. 1996. Computational methods for fluid dynamics. Springer Berlin, 356p.
[131] Tominaga Y. 2015. Flow around a high-rise building using steady and unsteady RANS CFD: Effect of large-scale fluctuations on the velocity statistics. J. Wind Eng. Ind. Aerodyn. 142: 93-103.
[132] Spalart PR, Allmaras SR. 1992. A one equation turbulence model for aerodynamic flows. AIAA Journal 94: 439.
[133] Jones, W., Launder, B. 1972. The prediction of laminarization with a two-equation model of turbulence. Int J Heat Mass Transfer 15: 301-14.
[134] Yakhot, V., and Orszag, S.A. Renormalization group analysis of turbulence. Journal of Scientific Computing 1986;1(1):3–51.
[135] Shih TH, Liou WW, Shabbir A, Zhu J. 1995. A new k-ε eddy-viscosity model for high Reynolds number turbulent flows – model development and validation. Comput Fluids 24 (3): 227-238.
[136] Wilcox, D. C. Turbulence modelling for CFD, 2nd Ed., DCW Industries, Inc; 2004.
[137] Menter, F. 1997. Eddy viscosity transport equations and their relation to the k–ε model. Journal of Fluids Engineering 119:876–884.

[138] Yuan C, Norford L, Britter R. Ng E. 2016. A modelling-mapping approach for fine-scale assessment of pedestrian-level wind in high-density cities. Building Environ 97: 152-165.
[139] Wood N. 2000. Wind flow over complex terrain: a historical perspective and the prospect for large-eddy modelling. Boundary Layer Meteorology 96: 11-32.
[140] Klein M. An attempt to assess the quality of large eddy simulations in the context of implicit filtering. Flow Turbulence Combust 2005; 75: 131-147.
[141] Celik I, Klein M, Janicka J. Assessment measures for engineering LES applications. J. Fluids Eng. 2009;131:10.
[142] Gousseau P, Blocken B, van Heijst GJF. 2013. Quality assessment of Large-Eddy Simulation of wind flow around a high-rise building: validation and solution verification. Comput Fluid 79: 120-133.
[143] Hanna, S.R., Plume dispersion and concentration fluctuations in the atmosphere. Encyclopedia of environmental control technology. In: Air Pollution Control, Vol. 2. Houston, TX: Gulf Publishing Company, 1989; 547–582.
[144] Kato, M., Launder, B.E. 1993. The modelling of turbulent flow around stationary and vibrating square cylinders. Nineth Symposium on Turbulent Shear Flows, pp. 10–14.
[145] Tominaga Y, Mochida A, Murakami S, Sawaki S. 2008b. Comparison of various revised k–ε models and LES applied to flow around a high-rise building model with 1:1:2 shape placed within the surface boundary layer. J Wind Eng Ind Aerodyn 96(4): 389-411.
[146] Yim SHL, Fung JCH, Lau AKH, Kot SC. 2009. Air ventilation impacts of the "wall effect" resulting from the alignment of high-rise buildings. Atmos Environ 43: 4982-4994.
[147] An K, Fung JCH, Yim SHL. 2013. Sensitivity of inflow boundary conditions on downstream wind and turbulence profiles through building obstacles using a CFD approach. J Wind Eng Ind Aerodyn 115: 137-149.
[148] Murakami, S., Mochida, A., Hibi, K. 1987. Three-dimensional numerical simulation of airflow around a cubic model by means of large eddy simulation. J Wind Eng Ind Aerodyn 25: 291–305.
[149] Murakami, S., Mochida, A., Hayashi, Y. 1990. Examining the k-ε model by means of a wind tunnel test and large-eddy simulation of the turbulence structure around a cube. J Wind Eng Ind Aerodyn 35, 87-100.
[150] Murakami, S., Mochida, A., Hayashi, Y., Sakamoto, S. 1992. Numerical study on velocity-pressure field and wind forces for bluff bodies by k-ε, ASM and LES. J Wind Eng Ind Aerodyn 44 (1-3), 2841-2852
[151] Murakami S. 1993. Comparison of various turbulence models applied to a bluff body. J Wind Eng Ind Aerodyn 46&47, 21-36.
[152] Murakami, S. 1998. Overview of turbulence models applied in CWE-1997. J Wind Eng Ind Aerodyn 74-76: 1-24.
[153] Murakami, S., Mochida, A. 1989. Three-dimensional numerical simulation of turbulent flow around buildings using the k−ε turbulence model. Building and Environment 24 (1), 51-64.
[154] Baetke F, Werner H, Wengle H. 1990. Numerical simulation of turbulent flow over surface-mounted obstacles with sharp edges and corners. J Wind Eng Ind Aerodyn 35(1-3), 129-147.
[155] Stathopoulos T, Baskaran A. 1990. Boundary treatment for the computation of 3D turbulent conditions around buildings. J Wind Eng Ind Aerodyn 35: 177–200.
[156] Cowan IR, Castro IP, Robins AG. 1997. Numerical considerations for simulations of flow and dispersion around buildings, J Wind Eng Ind Aerodyn 67 & 68: 535-545.
[157] Hall, R.C. (ed.). 1997. Evaluation of modelling uncertainty. CFD modelling of near-field atmospheric dispersion. Project EMU final report, European Commission Directorate–General XII Science, Research and Development Contract EV5V-CT94- 0531. Surrey: WS Atkins Consultants Ltd.
[158] Schatzmann M, Rafailidis S, Pavageau M. 1997. Some remarks on the validation of small-scale dispersion models with field and laboratory data. J Wind Eng Ind Aerodyn 67-68: 885-893.
[159] Menter, F., Hemstrom, B., Henrikkson, M., Karlsson, R., Latrobe, A., Martin, A., Muhlbauer, P., Scheuerer, M., Smith, B., Takacs, T., Willemsen, S. 2002. CFD Best Practice Guidelines for CFD Code Validation for Reactor-Safety Applications, Report EVOLECORA-D01, Contract No. FIKS-CT-2001-00154, 2002.
[160] Scaperdas, A., Gilham, S., 2004. Thematic Area 4: Best practice advice for civil construction and HVAC, The QNET-CFD Network Newsletter 2(4), 28-33.
[161] Bartzis JG, Vlachogiannis D, Sfetsos A. 2004. Thematic area 5: Best practice advice for environmental flows. The QNET-CFD Network Newsletter 2(4): 34-39.
[162] Britter R, Schatzmann M. (Eds.). 2007. Model Evaluation Guidance and Protocol Document COST Action 732. COST Office Brussels, ISBN 3-00-018312-4.
[163] Tamura, T., Nozawa, K., Kondo, K. 2008. AIJ guide for numerical prediction of wind loads on buildings. Journal of Wind Engineering and Industrial Aerodynamics, 96 (10-11), 1974-1984.
[164] Jakeman AJ, Letcher RA, Norton JP. 2006. Ten iterative steps in development and evaluation of environmental models. Environ Modell Softw 21(5): 602-614.

[165] Robson, B.J., Hamilton, D.P., Webster, I.T., Chan, T. 2008. Ten steps applied to development and evaluation of process-based biogeochemical models of estuaries. Environmental Modelling & Software, 23, 4, 369-384.
[166] Roache PJ. 1994. Perspective: a method for uniform reporting of grid refinement studies. J Fluids Eng 116: 405-413.
[167] Roache PJ. 1997. Quantification of uncertainty in computational fluid dynamics. Annu. Rev. Fluid Mech. 29: 123-160.
[168] AIAA. 1998. Guide for the verification and validation of computational fluid dynamics simulations, American Institute of Aeronautics and Astronautics, AIAA, AIAA-G-077-1998, Reston, VA
[169] Oberkampf WL, Trucano TG, Hirsch C. 2004. Verification, validation, and predictive capability in computational engineering and physics. Appl Mech Rev 57(5): 345-384.
[170] Roy CH. 2005. Review of code and solution verification procedures for computational simulation. J Comput Phys 205: 131-156.
[171] Roy, C.J, Oberkampf, W.L. 2010. A complete framework for verification, validation, and uncertainty quantification in scientific computing. 48th AIAA Aerospace Sciences Meeting Including the New Horizons Forum and Aerospace Exposition 4 - 7 January 2010, Orlando, Florida.
[172] ASME, 2009. Standard for verification and validation in Computational Fluid Dynamics and heat transfer. ASME V&V 20-2009, The American Society of Mechanical Engineers.
[173] ASME 2011. http://journaltool.asme.org/Templates/JFENumAccuracy.pdf. Retrieved on 30 July 2011.
[174] Roache PJ, Chia KN, White F. 1986. Editorial policy statement on the control of numerical accuracy. J Fluids Eng 108:2
[175] Freitas CJ. 1993. J. Fluids Eng. editorial policy statement on the control of numerical accuracy. J Fluids Eng 115: 339-340.
[176] Richards PJ, Hoxey RP. 1993. Appropriate boundary conditions for computational wind engineering models using the k-ε turbulence model. J Wind Eng Ind Aerodyn 46&47: 145-153.
[177] Hargreaves DM, Wright N.G. 2007. On the use of the k–ε model in commercial CFD software to model the neutral atmospheric boundary layer. J Wind Eng Ind Aerodyn 95(5): 355-369.
[178] Blocken B, Stathopoulos T, Carmeliet J. 2007b. CFD simulation of the atmospheric boundary layer: wall function problems. Atmos Environ 41(2): 238-252.
[179] Gorlé C, van Beeck J, Rambaud P, Van Tendeloo G. 2009. CFD modelling of small particle dispersion: the influence of the turbulence kinetic energy in the atmospheric boundary layer. Atmos Environ 43(3): 673-681.
[180] Yang Y, Gu M, Chen S, Jin X. 2009. New inflow boundary conditions for modelling the neutral equilibrium atmospheric boundary layer in computational wind engineering. J Wind Eng Ind Aerodyn 97(2): 88-95.
[181] Parente A, Gorlé C, van Beeck J, Benocci C. 2011. Improved k-ε model and wall function formulation for the RANS simulation of ABL flows. J Wind Eng Ind Aerodyn 99(4): 267-278.
[182] Richards PJ, Norris SE. 2011. Appropriate boundary conditions for computational wind engineering models revisited. J Wind Eng Ind Aerodyn 99(4): 257-266.
[183] Tucker PG, Mosquera A. 2001. NAFEMS introduction to grid and mesh generation for CFD. NAFEMS CFD Working Group, R0079, 56 pp.
[184] van Hooff T, Blocken B. 2010a. Coupled urban wind flow and indoor natural ventilation modelling on a high-resolution grid: A case study for the Amsterdam ArenA stadium. Environ Modell Softw 25 (1): 51-65.
[185] Schatzmann M, Leitl B. 2011. Issues with validation of urban flow and dispersion CFD models. J Wind Eng Ind. Aerodyn 99(4): 169-186.
[186] Ferziger JH. 1993. Estimation and reduction of numerical error. FED Vol. 158, Symposium on Quantification of Uncertainty in Computational Fluid Dynamics, ASME Fluid Engineering Division, Summer Meeting, Washington DC, June 20-24, pp. 1-8.
[187] Castro IP, Graham JMR. 1999. Numerical wind engineering: the way ahead? Proceedings of the Institution of Civil Engineers – Structures and Buildings, 134, 3, 275-277.
[188] Tominaga, Y., Stathopoulos, T. 2013. CFD simulation of near-field pollutant dispersion in the urban environment: A review of current modelling techniques. Atmos Environ 79, 716-730.
[189] Blocken B, Tominaga Y, Stathopoulos T. 2013. CFD simulation of micro-scale pollutant dispersion in the built environment. Build Environ 64: 225–230.
[190] Lateb M, Meroney RN, Yataghene M, Fellouah H, Saleh F, Boufadel MC. 2015. On the use of numerical modelling for near-field pollutant dispersion in urban environments – A review. Environmental Pollution. In press. doi:10.1016/j.envpol.2015.07.039
[191] Hanjalic, K., 2004. Will RANS survive LES? A view of perspectives. Journal of Fluids Engineering – Transactions of the ASME 127, 5, 831-839.

[192] Baker C.J., 2007. Wind engineering – Past, present and future. Journal of Wind Engineering and Industrial Aerodynamics 95(9-11), 843-870.
[193] Iaccarino G. 2009. Introduction to uncertainty representation and propagation. Tech. rep. Neuilly-sur-Seine, France: NATO Research and Technology Organization.
[194] Garcia-Sanchez C, Philips DA, Gorlé C. 2014. Quantifying inflow uncertainties for CFD simulations of the flow in downtown Oklahoma City. Build Environ 78: 118-129.
[195] Gorlé C, Garcia-Sanchez C, Iaccarino G. 2015. Quantifying inflow and RANS turbulence model form uncertainties for wind engineering flows. J Wind Eng Ind Aerodyn 144: 202-212.
[196] Ferziger, J.H. 1990. Approaches to turbulent flow computation: applications to flow over obstacles. Journal of Wind Engineering and Industrial Aerodynamics 35: 1-19.
[197] Walter B, Horender S, Voegeli C, Lehning M. 2014. Experimental assessment of Owen's second hypothesis on surface shear stress induced by a fluid during sediment saltation. Geophysical Research Letters 41(17): 6298-6305.

Table 1: Criteria for wind comfort according to NEN 8100 [19]

$P(U_{THR} > 5$ m/s (in % hours per year)	Grade	Activity		
		Traversing	Strolling	Sitting
< 2.5	A	Good	Good	Good
2.5 – 5.0	B	Good	Good	Moderate
5.0 – 10	C	Good	Moderate	Poor
10 – 20	D	Moderate	Poor	Poor
> 20	E	Poor	Poor	Poor

Table 2: Criteria for wind danger according to NEN 8100 [19]

$P(U_{THR} > 15$ m/s (in % hours per year)	Grade	Activity		
		Traversing	Strolling	Sitting
0.05 - 0.30	Limited risk	Acceptable	Not acceptable	Not acceptable
≥ 0.30	Dangerous	Not acceptable	Not acceptable	Not acceptable

Table 3. Different wind comfort and wind danger criteria consisting of wind speed thresholds and maximum allowed exceedance probabilities for different pedestrian activity categories [18].

Reference	**Threshold (moderate/tolerable wind climate)**	**P_{max}**	**Description of activity**
***A (Sitting long)**: Sitting for a long period of time, laying in steady position, pedestrian sitting, terrace, street café or restaurant, open field theatre, pool*			
Isyumov & Davenport [20]	U > 3.6 m/s (3 Bft)	1.5 % (1/week)	"Tolerable climate for sitting - long exposure (outdoor restaurants, bandshells, theatres)"
Lawson [21]	U > 1.8 m/s (2 Bft)	2 %	"Tolerable for covered areas"
Melbourne [22]	$U + 3.5\sigma_u > 10$ m/s	0.022% (2h/year)	"Generally acceptable for stationary, long-exposure activities (outdoor restaurants, theatres)"
NEN 8100 [19]	U > 5 m/s	2.5 %	Quality Class A: "good climate for sitting long (parks)". Note: the Dutch Standard does not focus on café or restaurant terraces
***B (Sitting short)**:Pedestrian standing, standing/sitting over a short period of time, short steady positions, public park, playing field, shopping street, mall*			
Isyumov & Davenport [20]	U > 5.3 m/s (4 Bft)	1.5% (1/week)	"Tolerable climate for standing, short exposure (parks, plaza areas)"
Lawson [21]	U > 3.6 m/s (3 Bft)	2 %	"Tolerable for pedestrian stand around"
Melbourne [22]	$U + 3.5\sigma_u > 13$ m/s	0.022% (2 h/year)	"Generally acceptable for stationary short-exposure activities (window shopping, standing or sitting in plazas)"
NEN 8100 [19]	U > 5 m/s	5 %	Quality Class B: "moderate climate for sitting long (parks)"
***C (Strolling)**: Pedestrian walking, leisurely walking, normal walking, ramble, stroll, walkway, building entrance, shopping street, mall*			
Isyumov & Davenport [20]	U > 7.6 m/s (5 Bft)	1.5 % (1/week)	"Tolerable climate for strolling, skating (parks, entrances, skating rinks)"
Lawson [21]	U > 5.3 m/s (4 Bft)	2 %	"Tolerable for pedestrian walk-thru"
Melbourne [22]	$U + 3.5\sigma_u > 16$ m/s	0.022% (2 h/year)	"Generally acceptable for main public access-ways"
NEN 8100 [19]	U > 5 m/s	10 %	Quality Class C: "moderate climate for strolling"
***D (Walking fast)**:Objective business walking, brisk or fast walking, car park, avenue, sidewalk, belvedere*			
Isyumov & Davenport [20]	U > 9.8 m/s (6 Bft)	1.5% (1/week)	"Tolerable for walking fast (sidewalks)"
Lawson [21]	U > 7.6 m/s (5 Bft)	2 %	"Tolerable for roads, car parks"
NEN 8100 [19]	U > 5m/s	20 %	Quality Class D: "moderate climate for walking fast"
Unacceptable, poor wind climate → *region in between D and Danger*			

Danger		**P_{min}**	
Isyumov & Davenport [20]	U > 15.1 m/s (U > 8 Bft)	0.01% (1/year)	"Dangerous"
Melbourne [22]	$U + 3.5\sigma_u > 23$ m/s	0.022% (2 h/year)	"Completely unacceptable – the gust speed at which people get blown over"
NEN 8100 [19]	U > 15 m/s	0.05 %	"limited risk" and "dangerous"

Table 4. Errors imposed on amplification factor K, yielding modified values K_{mod}.

K	Error	K_{mod}
2.0	10%	1.8
1.9	10%	1.71
1.8	10%	1.62
1.7	10%	1.53
1.6	10%	1.44
1.5	10%	1.35
1.4	10%	1.26
1.3	10%	1.17
1.2	10%	1.08
1.1	10%	0.99
1.0	20%	0.8
0.9	20%	0.72
0.8	30%	0.56
0.7	30%	0.49
0.6	50%	0.3
0.5	50%	0.25
0.4	70%	0.12
0.3	70%	0.09
0.2	90%	0.02
0.1	90%	0.01

Table 5. Amplification factors K and K_{mod} for points A and B and all wind directions.

	POINT A		POINT B	
	K	K_{mod}	K	K_{mod}
0°	2.00	1.80	1.50	1.35
30°	1.80	1.62	1.50	1.35
60°	1.50	1.35	1.20	1.08
90°	0.90	0.72	1.40	1.26
120°	1.20	1.08	1.40	1.26
150°	1.80	1.62	0.90	0.72
180°	2.00	1.80	1.00	0.80
210°	1.50	1.35	1.00	0.80
240°	1.20	1.08	1.50	1.35
270°	1.20	1.08	1.50	1.35
300°	1.20	1.08	1.20	1.08
330°	1.80	1.62	1.50	1.35

Table 6. Total exceedance probabilities for amplification factors K and K_{mod} for points A and B and for different values of U_{THR}.

U_{THR}	U_{THR} = 1 m/s		U_{THR} = 3 m/s		U_{THR} = 5 m/s		U_{THR} = 8 m/s		U_{THR} = 10 m/s	
	A	B	A	B	A	B	A	B	A	B
P(K)	91.1	89.8	54.1	45.5	20.8	12.3	3.1	0.7	0.7	0.1
P(K_{mod})	89.5	87.3	47.1	36.2	15.2	7.6	1.6	0.3	0.2	0.0
Difference	1.6	2.5	6.9	9.3	5.6	4.7	1.5	0.5	0.4	0.0

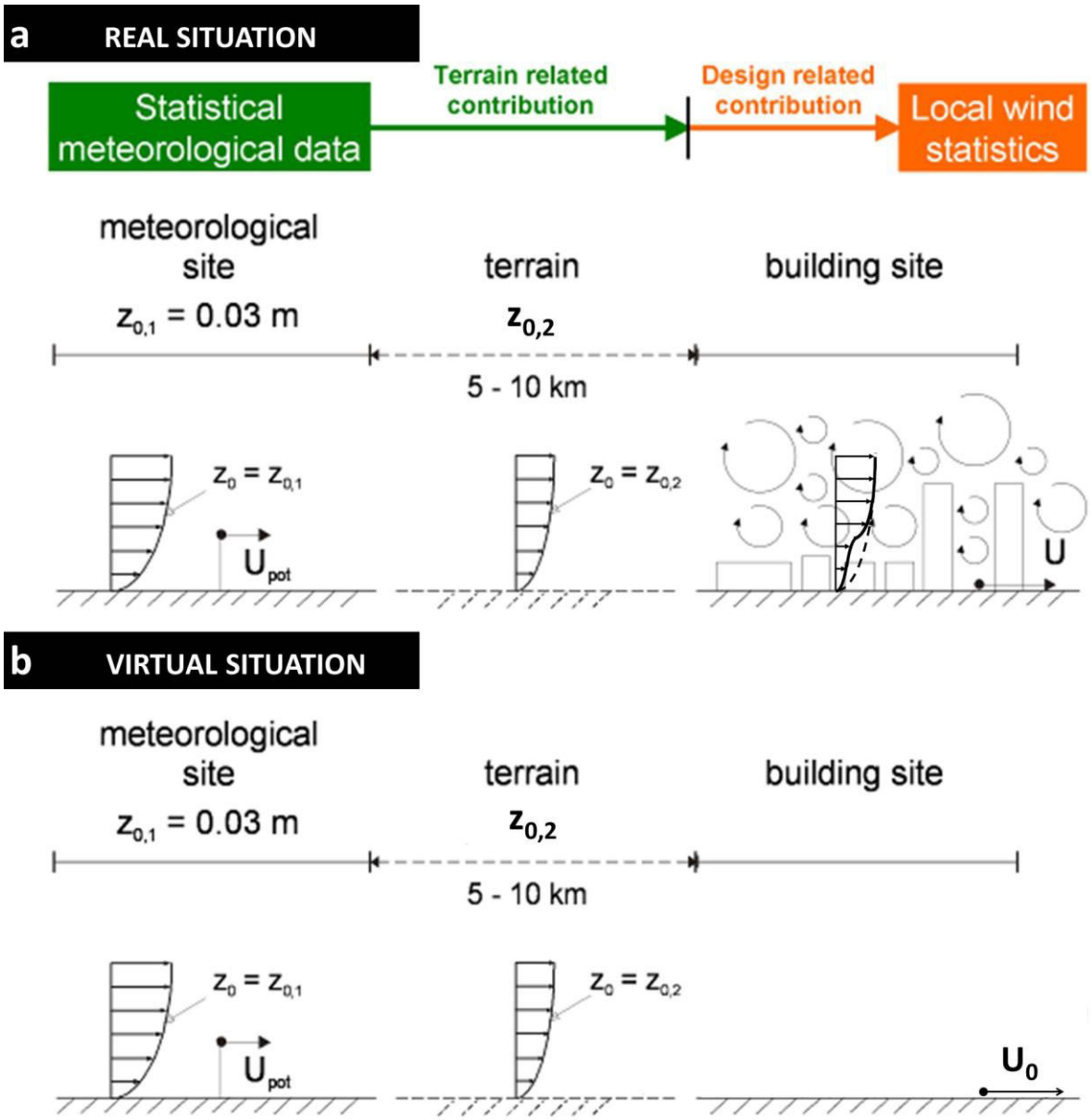

Figure 1. (a) Schematic representation of transformation of statistical meteorological data from the meteorological site to the building site, with indication of the wind speed at the meteorological station (U_{pot}) and the wind speed at the location of interest (U). (b) The reference wind speed at the building site (U_0) is defined in the virtual situation as the wind speed at the location of interest but without buildings present. The corresponding aerodynamic roughness lengths z_0 are also indicated.

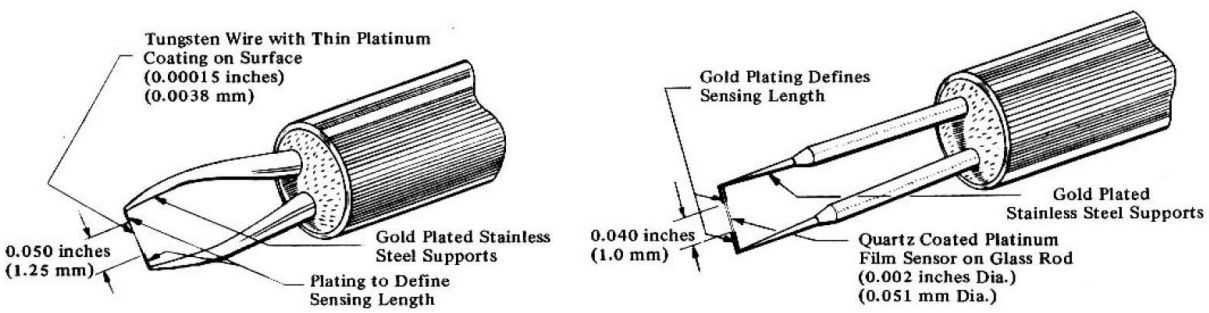

Figure 2. Hot-wire and hot-film anemometry sensors (Source unknown)

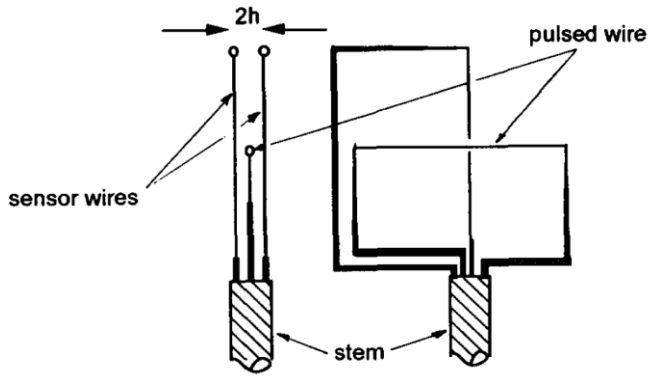

Figure 3. Pulsed- Pulsed-wire velocity probe geometry [103]. Wire lengths (l) typically 5-10 mm; wire spacing (h) typically 0.5-1.5 mm.

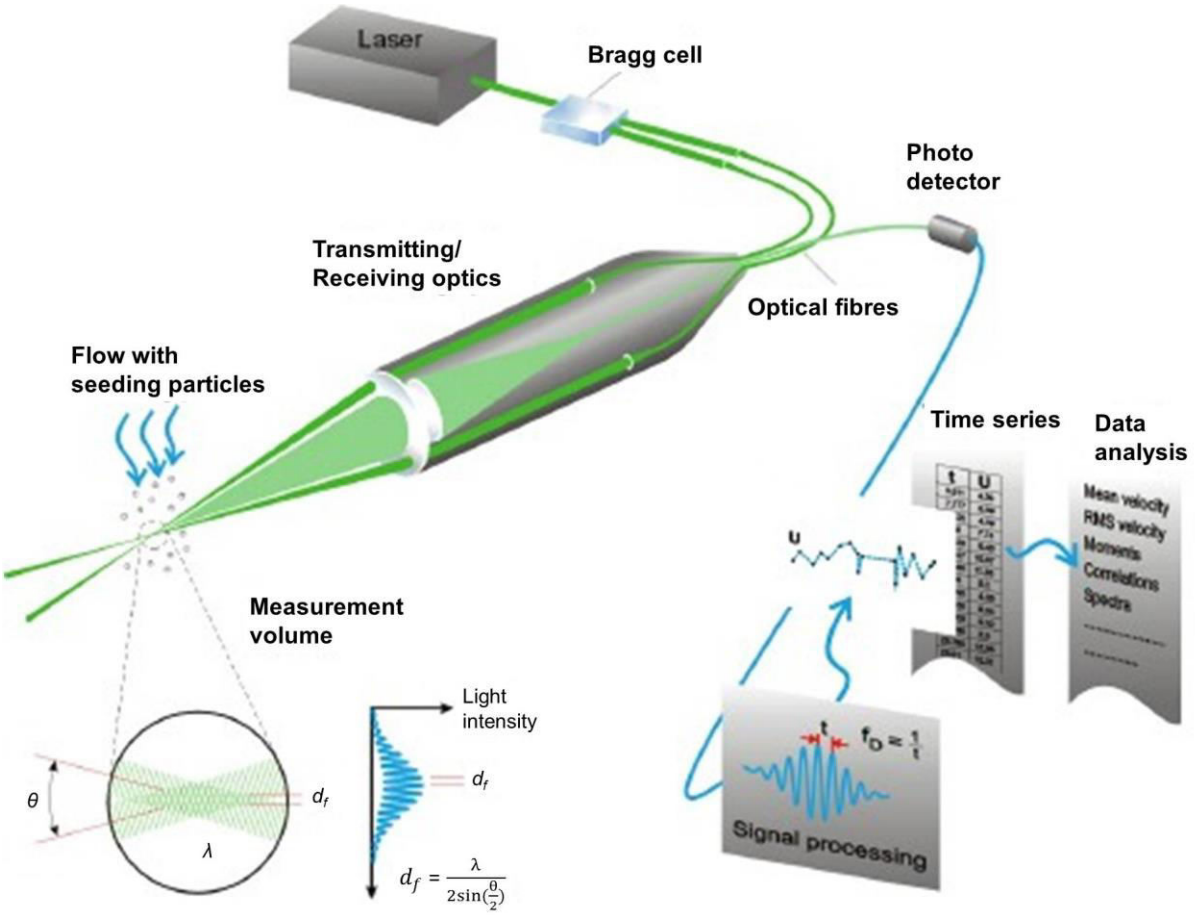

Figure 4. Measurement principle of laser-Doppler anemometry (modified from www.DantecDynamics.com).

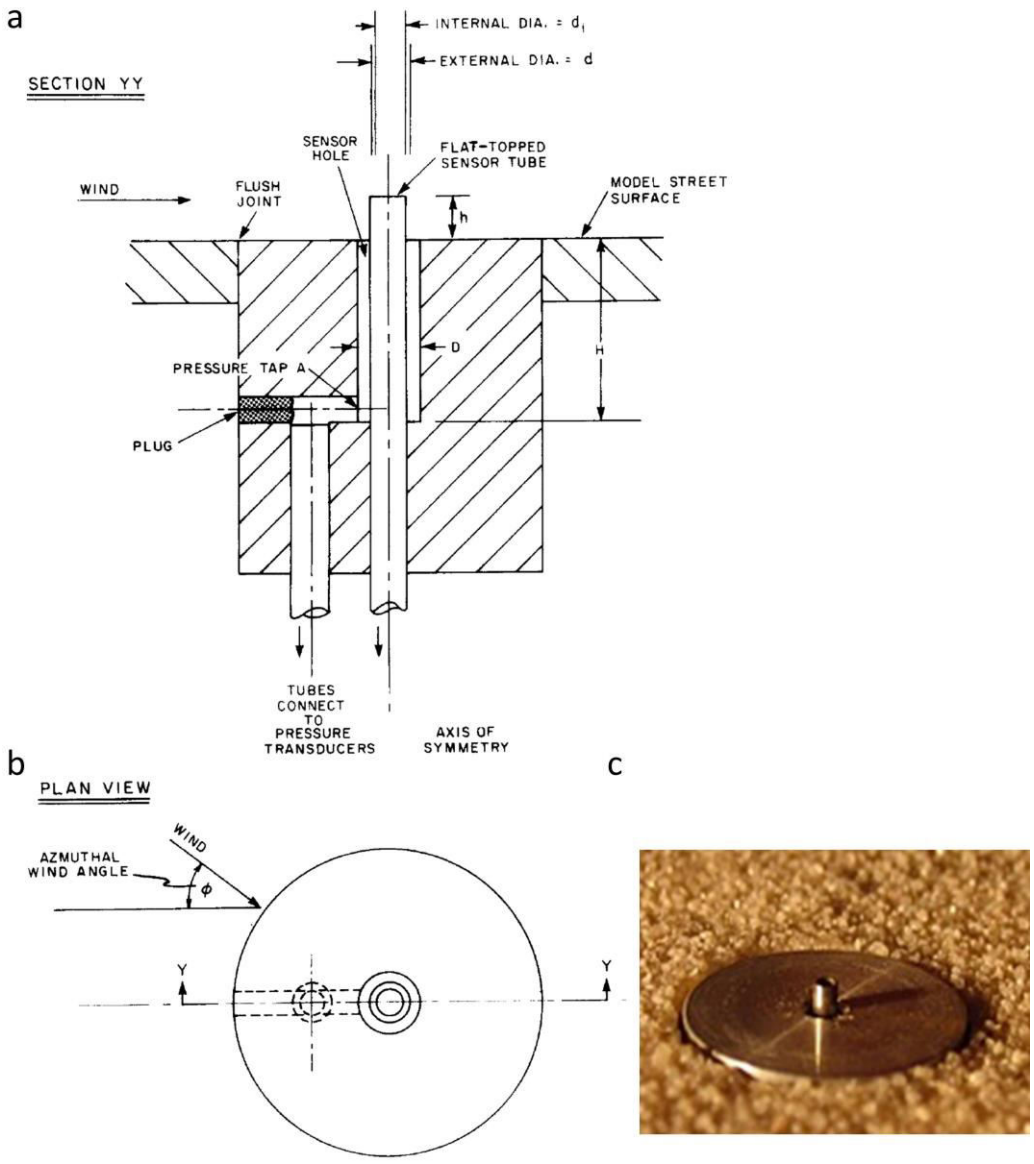

Figure 5. Irwin sensor [37,197].

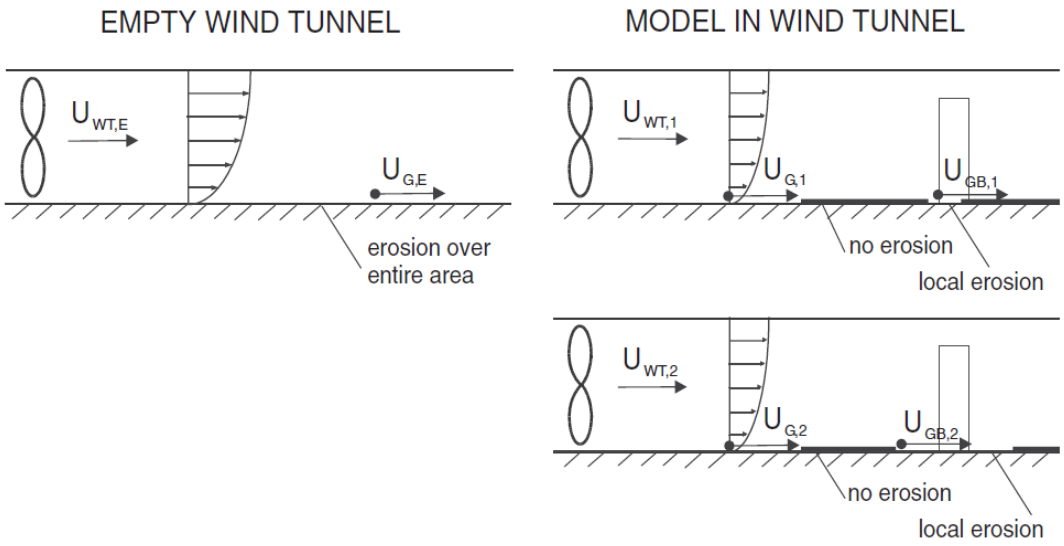

Figure 6. Schematic representation of sand erosion technique.

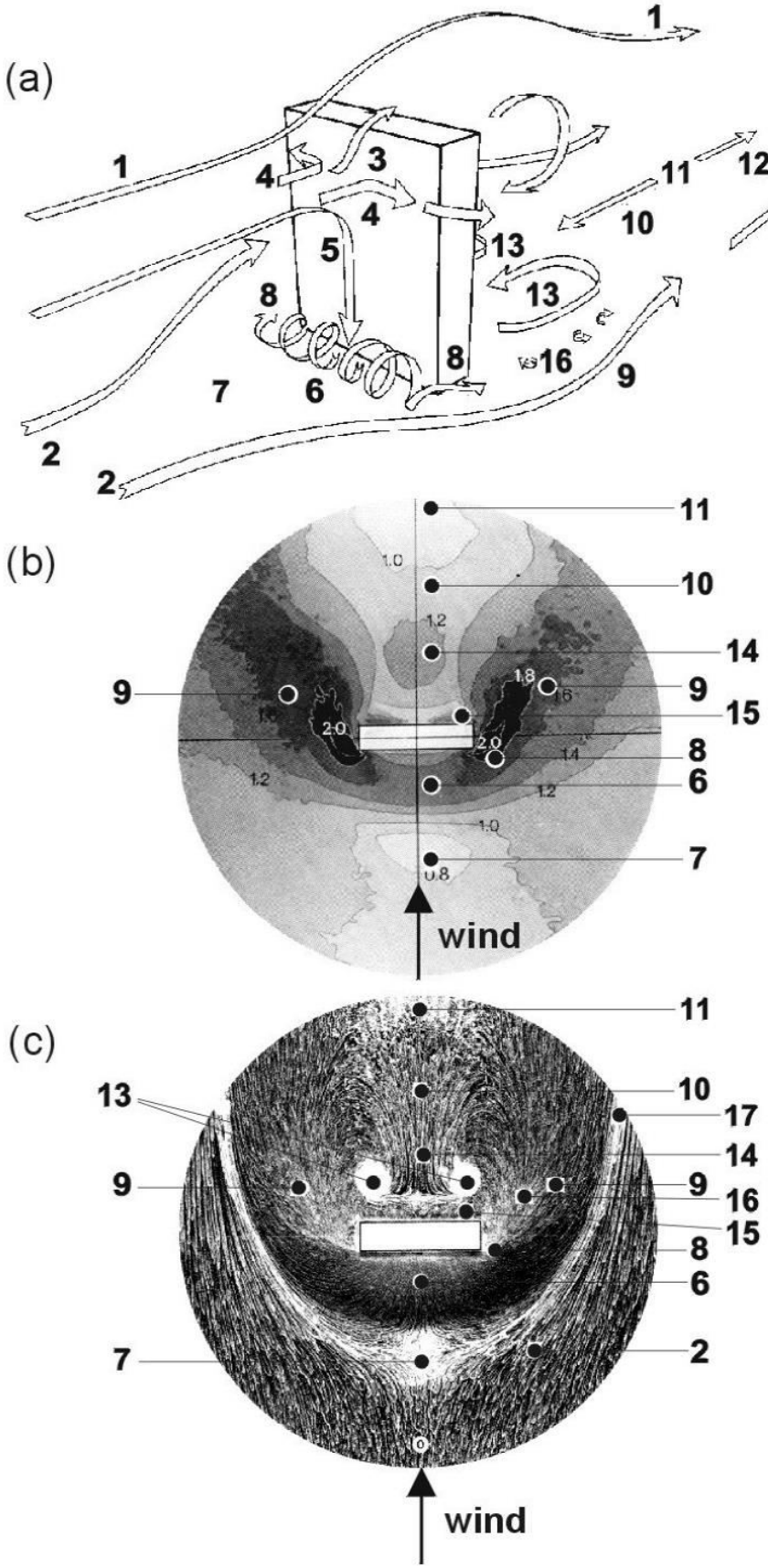

Figure 7. Wind flow around a single wide high-rise rectangular building with full-scale dimensions L x B x H = 80 x 20 x 70 m³ : (a) schematic representation; (b) sand erosion contour plot; and (c) kaoline streak line plot obtained from wind tunnel tests (modified from [44]).

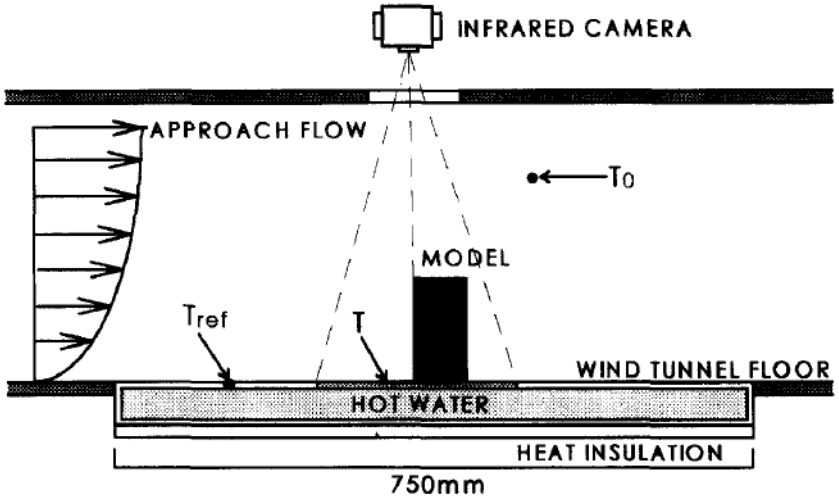

Figure 8. Set-up for assessing PLW by infrared thermography [52].

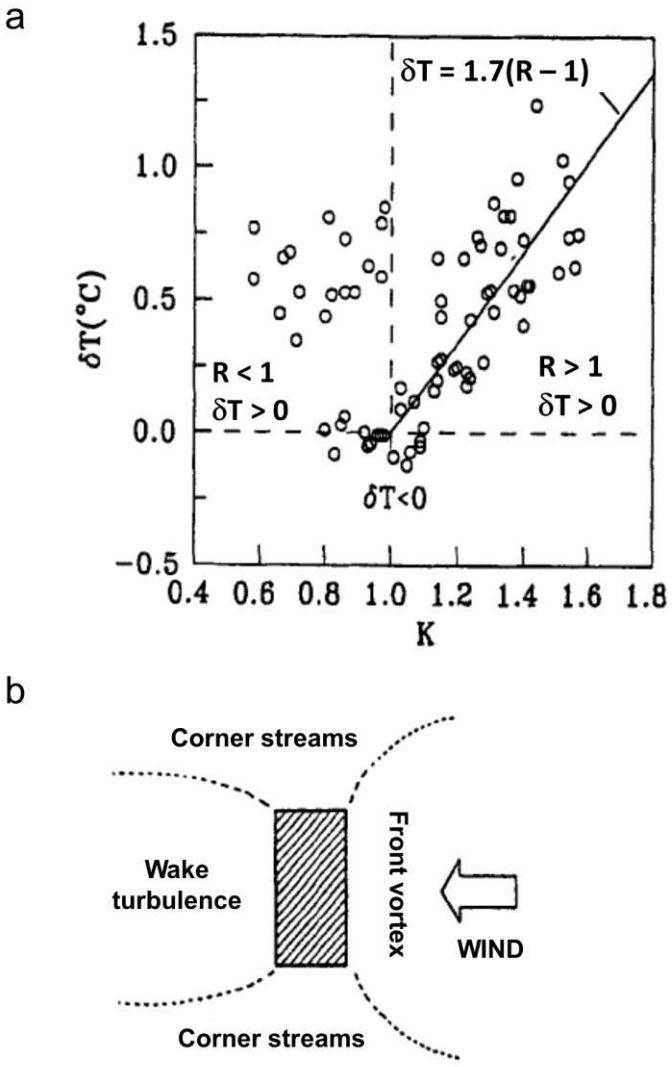

Figure 9. (a) Surface temperature reduction as a function of local amplification factor. (b) Schematic division of the surface around a building model in three zones (modified from [51]).

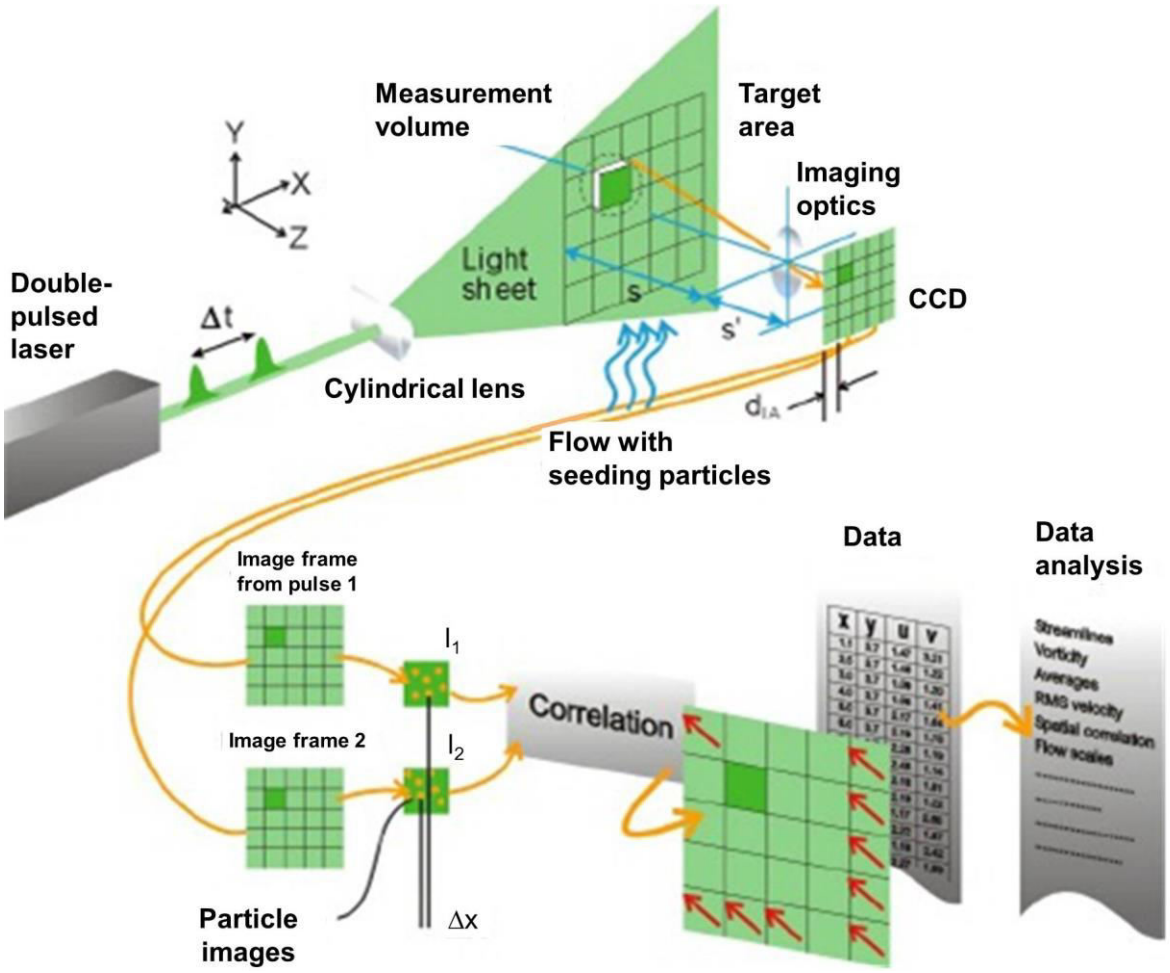

Figure 10. Measurement principle of particle image velocimetry (modified from www.DantecDynamics.com).

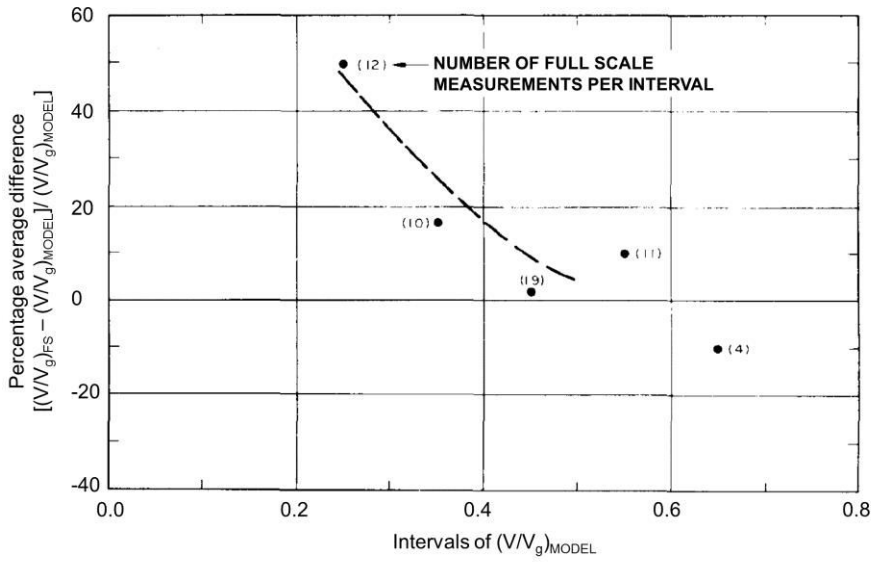

Figure 11. Average differences between full-scale and wind tunnel mean plaza wind speed ratios [23].

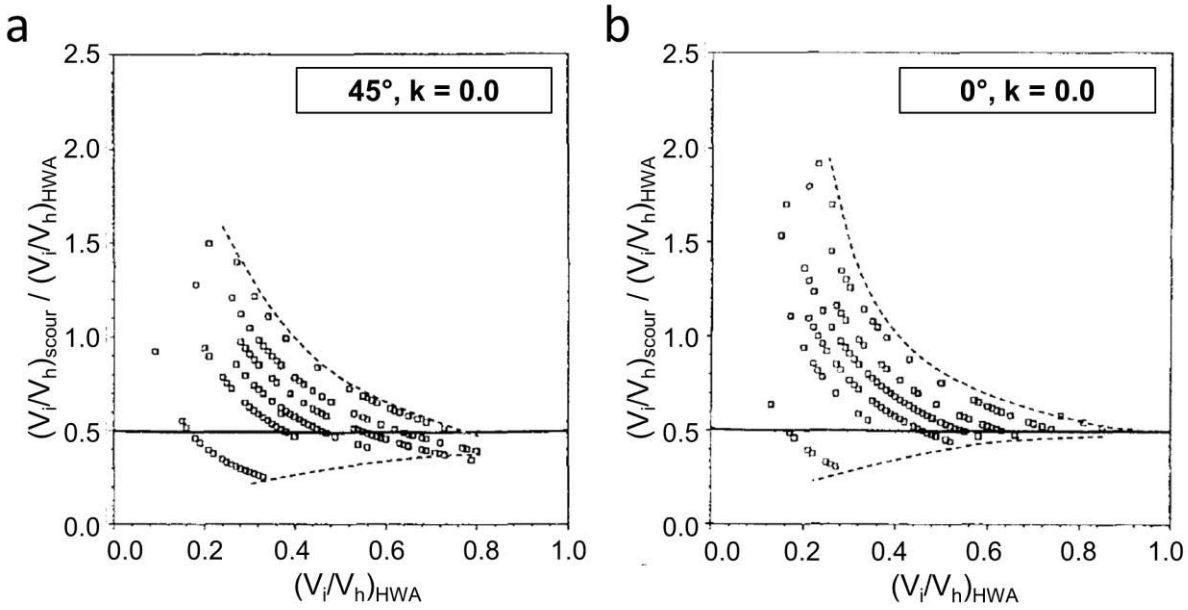

Figure 12. Comparison of wind speed ratios from scour tests with HWA, for wind angle 45 and 0° [47].

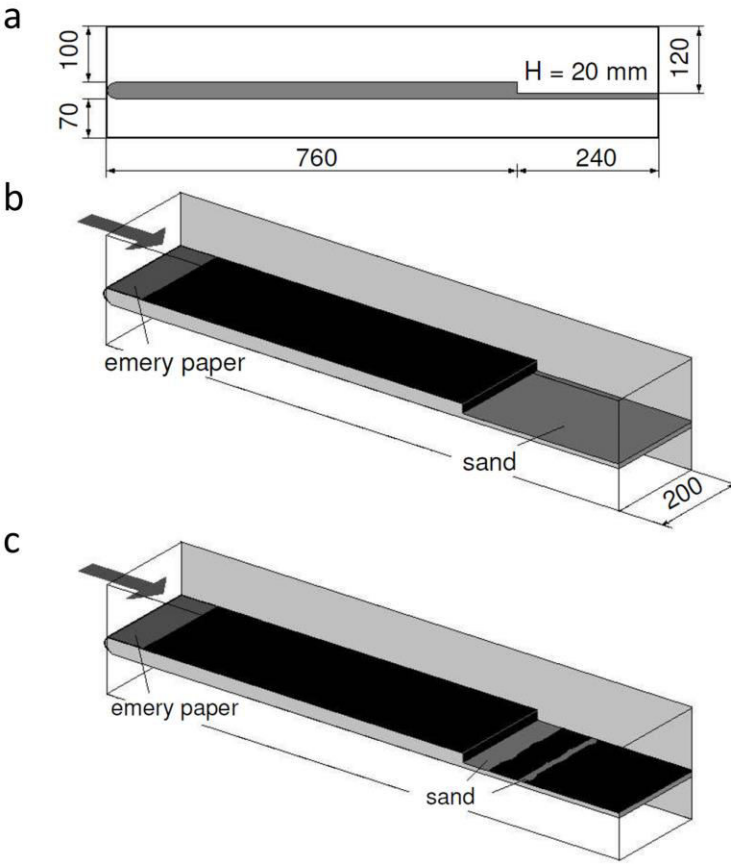

Figure 13. Experimental setup of backward facing step for sand-erosion tests: (a) Vertical cross-section with dimensions in mm; (b-c) Perspective view with position of emery paper and sand layer (b) before and (c) after erosion (modified from [107]).

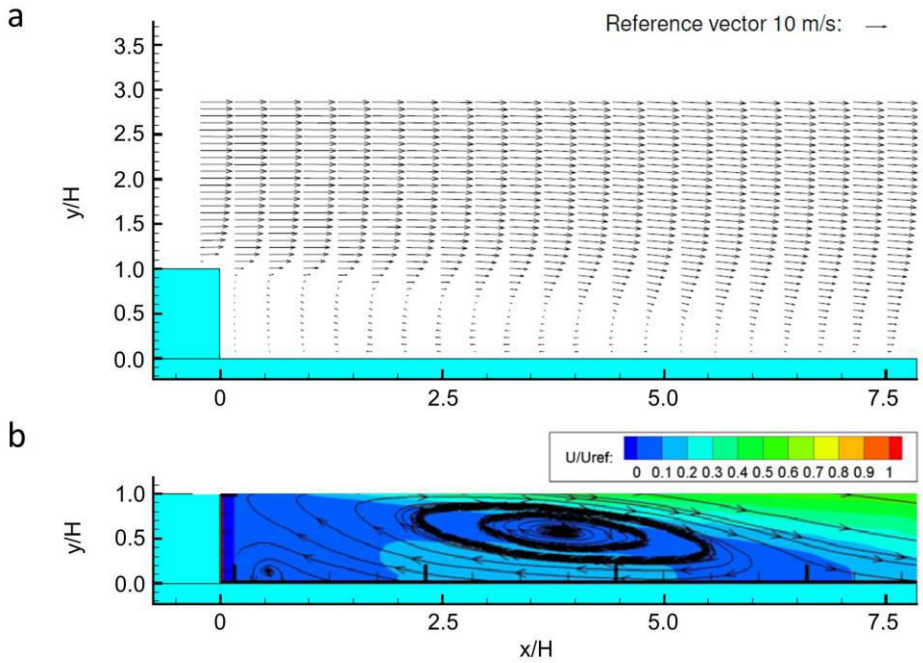

Figure 14. PIV measurement results of flow over backward-facing step: (a) Velocity-vector field; (b) Streamlines and wind speed contours (modified from [49] and [107]).

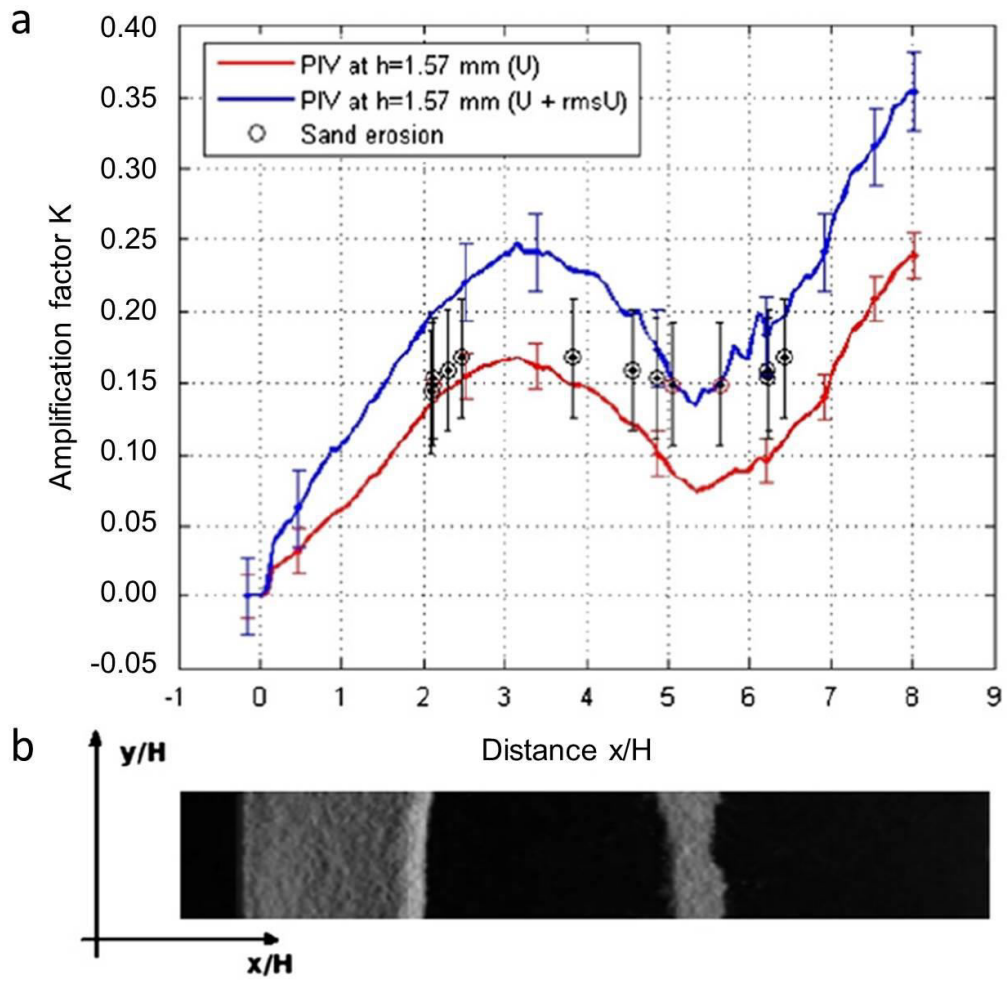

Figure 15. (a) Comparison of amplification factor K computed from PIV measurements and from sand-erosion tests (modified from [49]); (b) Top view of the sand-erosion pattern after 1 min. at 17 m/s.

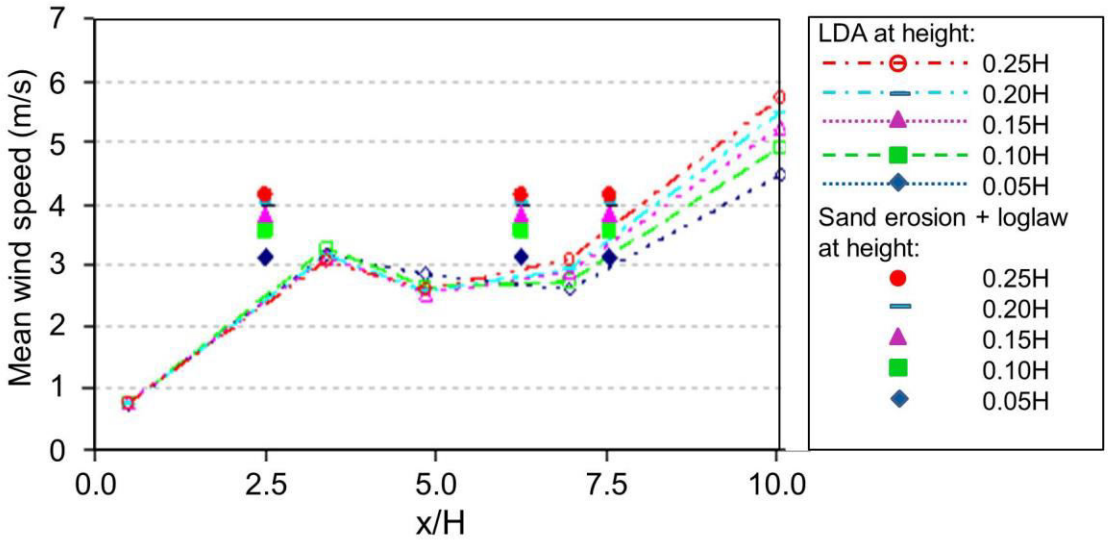

Figure 16. Comparison of mean wind speed downstream of backward facing step, obtained by LDA and sand erosion in combination with the log law profile, at different heights above the wind tunnel floor (modified from [41])

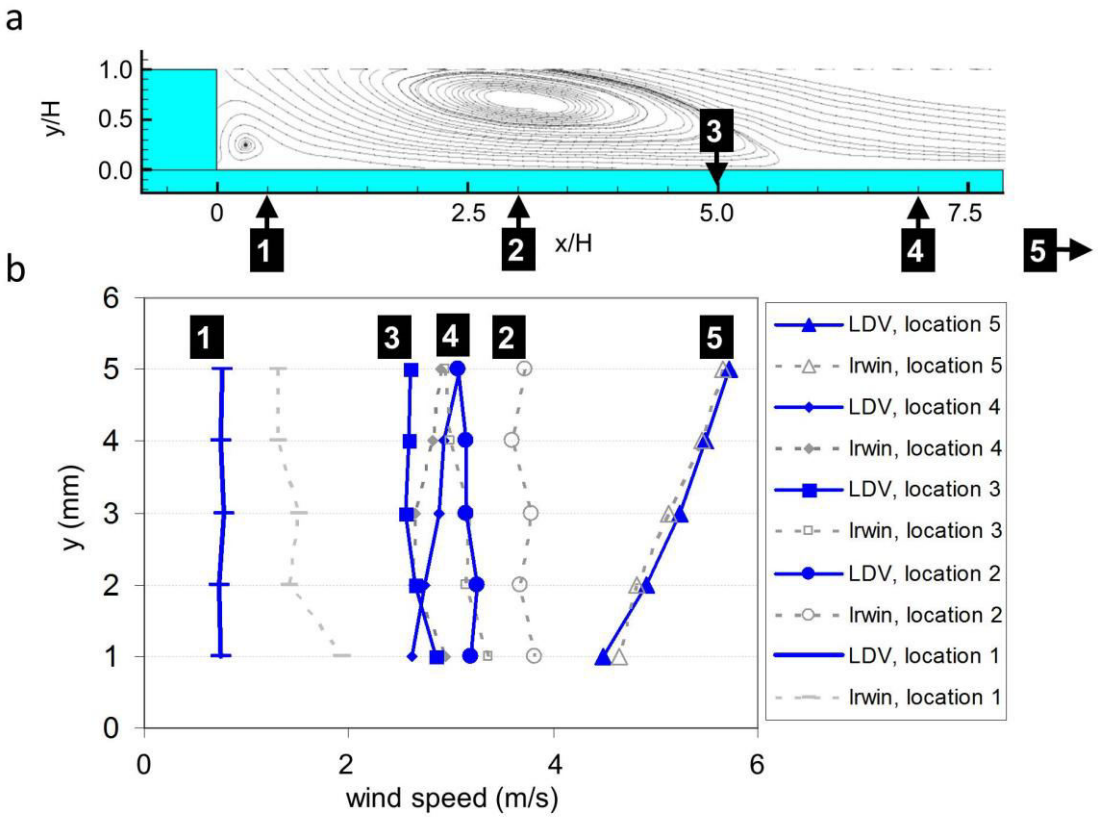

Figure 17. (a) Streamlines downstream of BFS with indication of the positions of Irwin probes and LDA measurements. (b) Comparison of mean wind speed from Irwin probes and LDA (modified from [41]).

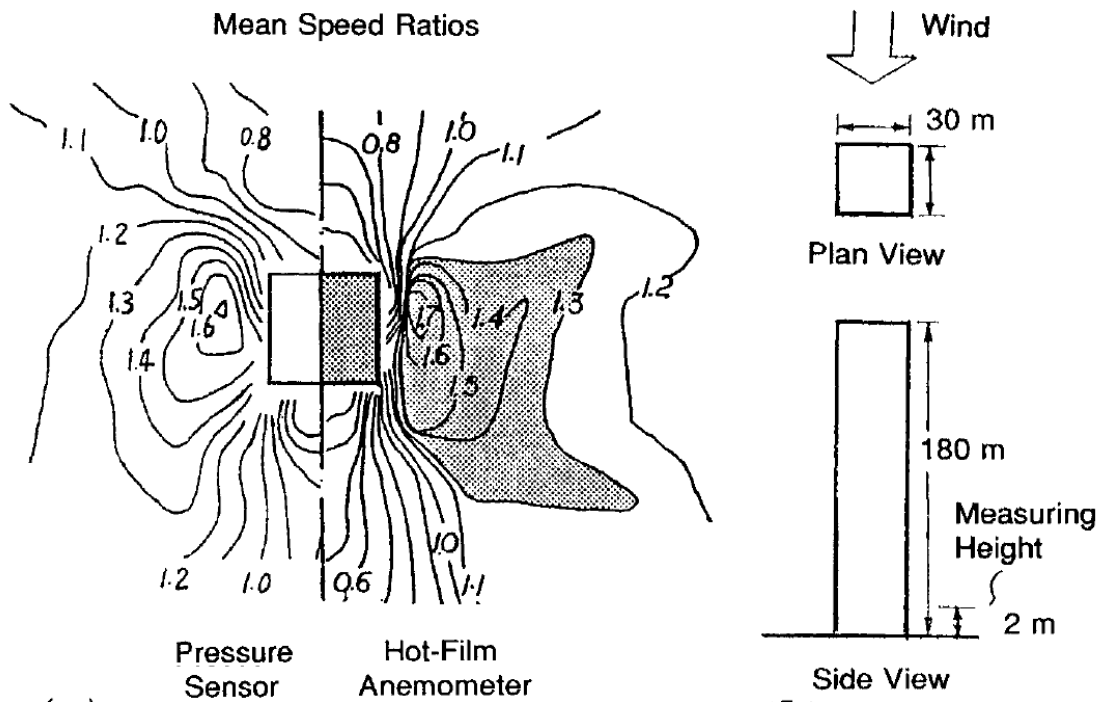

Figure 18. Comparison of amplification ratios of mean and RMS wind speed between Irwin probe and HFA [91].

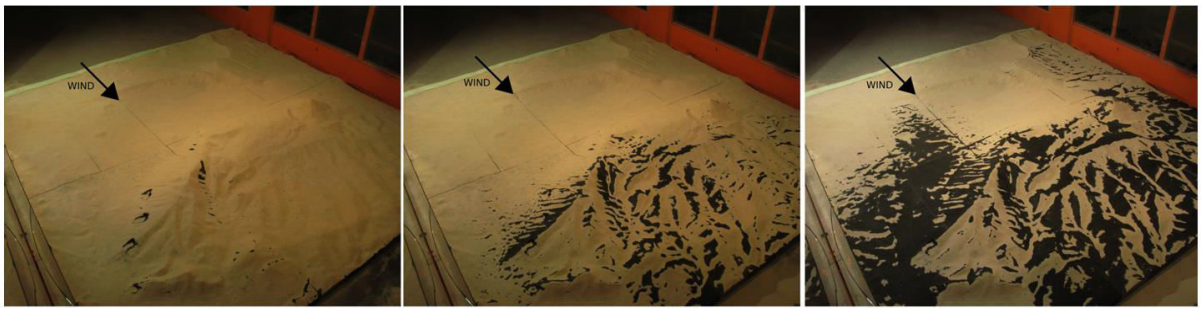

Figure 19. Sand erosion test for wind park site assessment on Alaiz mountain, Spain. Scaling factor is 5300. (a) Beginning of test. (b) After 60 s at 6 m/s. (c) After 60 s at 7 m/s [49].

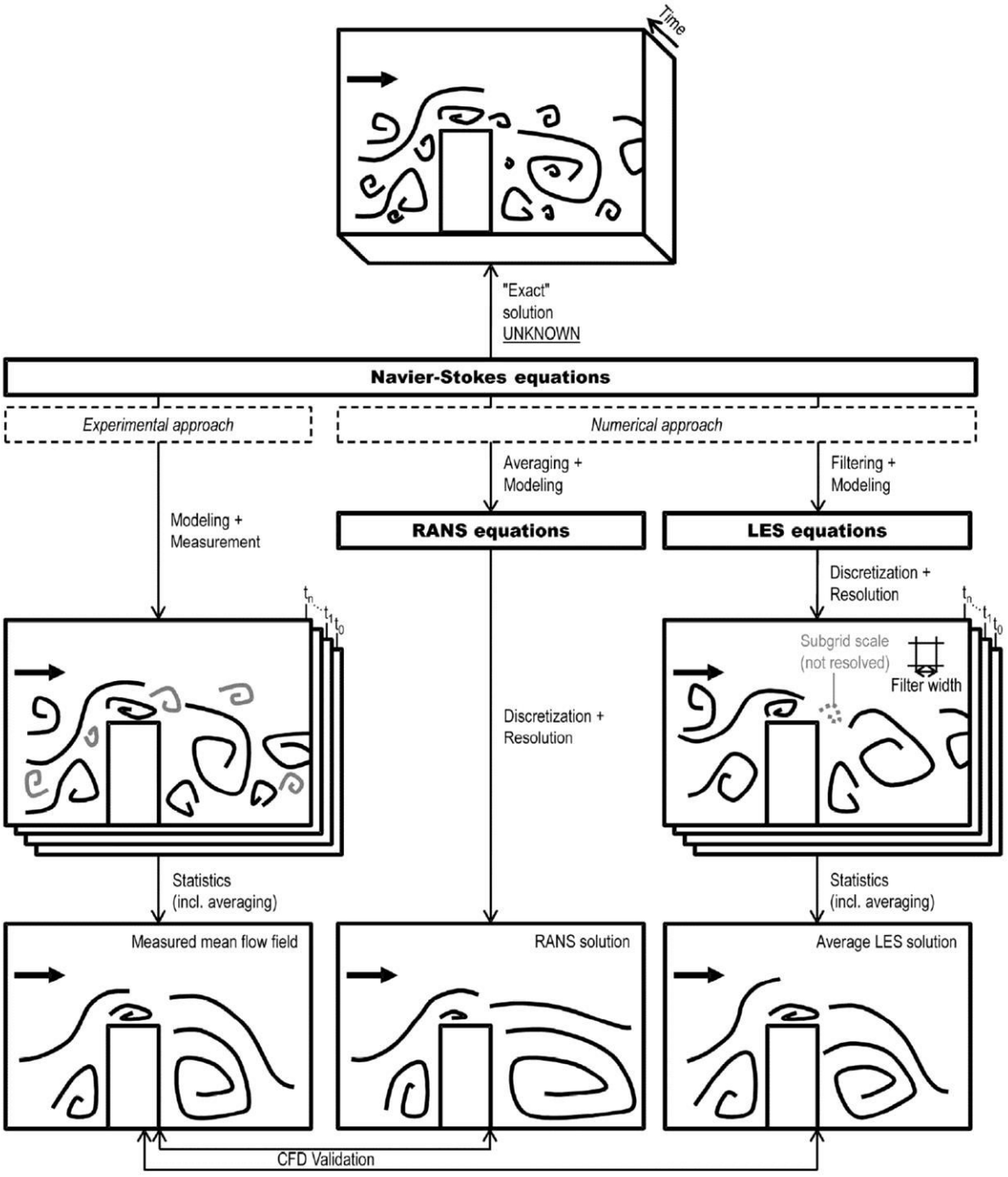

Figure 20. Schematic representation of flow around a building as captured by experiments, RANS and LES simulations (courtesy of P. Gousseau).

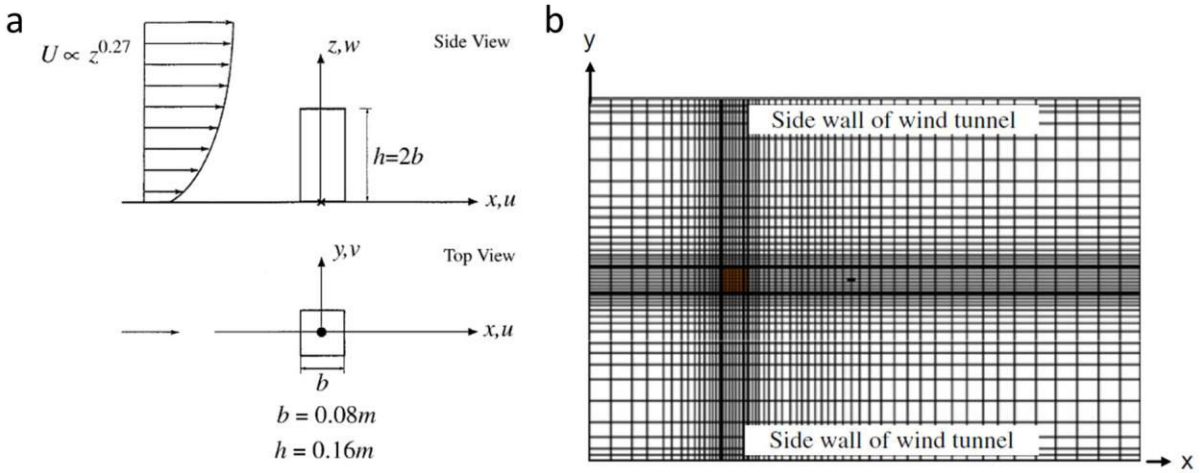

Figure 21. Building configuration in the validation studies by Yoshie et al. [75], (a-b) Geometry and structured grid ($1.0x10^5$ cells) of isolated building.

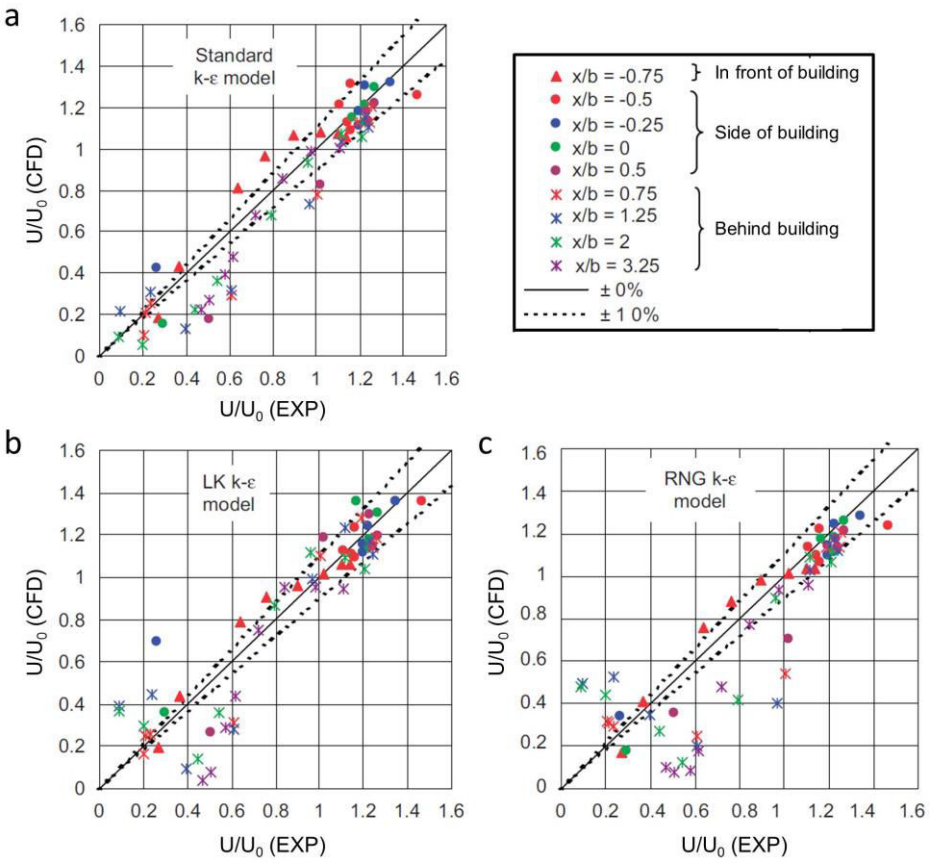

Figure 22. Comparison of CFD results and wind tunnel measurements of wind speed ratio for the isolated building (see Figure 4a) by Yoshie et al. [75], (a) steady RANS with standard k-ε model, (b) steady RANS with LK k-ε model, (c) steady RANS with RNG k-ε model. The symbols refer to: Δ = front of building; o = side of building; x = behind building. The different colors refer to a variety of positions in front, beside and behind the building.

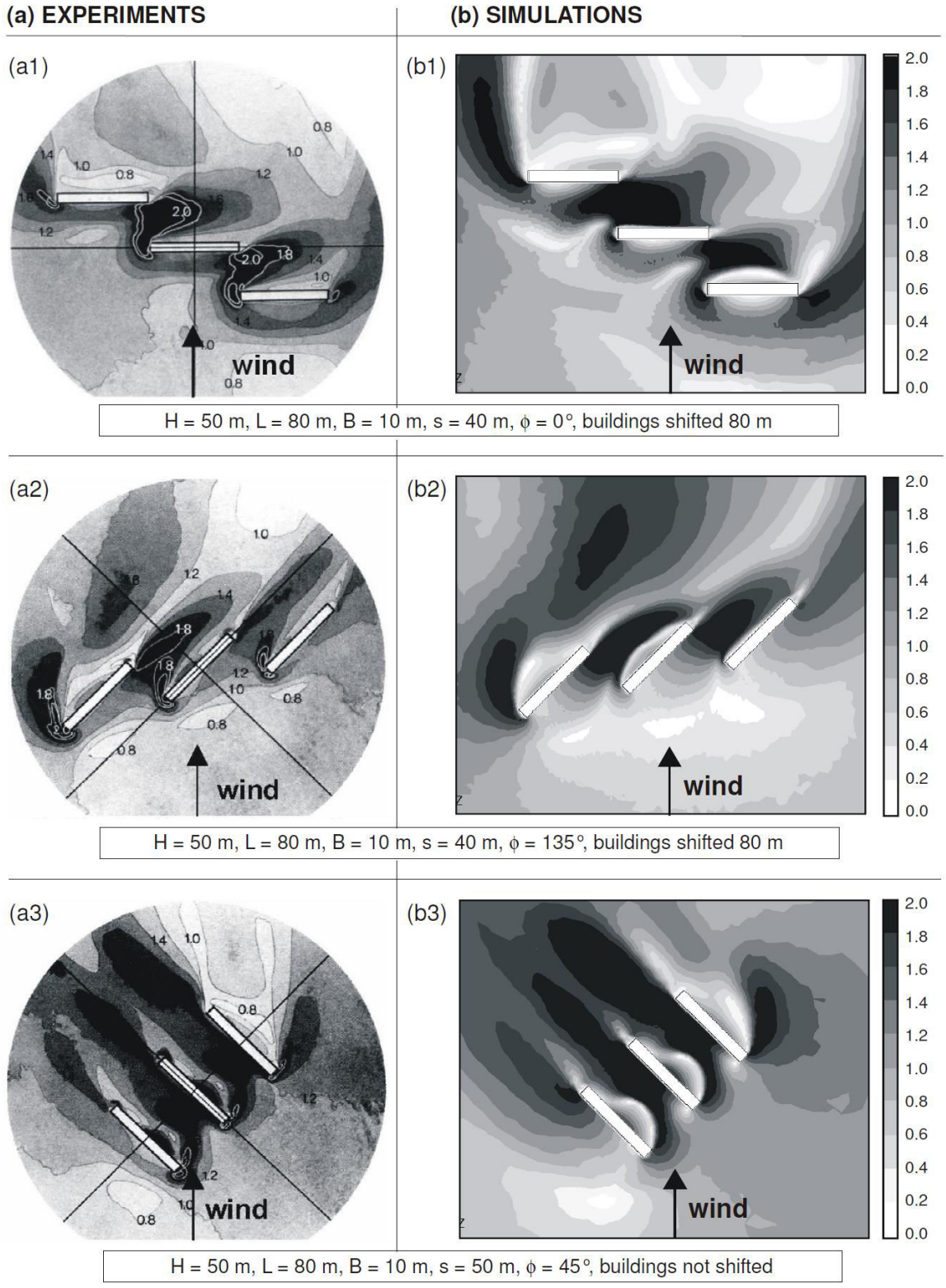

Figure 23. Validation study for parallel building configurations by Blocken and Carmeliet [68], (a) Sand-erosion contour plots versus (b) CFD results of the amplification factor K. White contour lines correspond to amplification factors of 1.8 and 2.0.

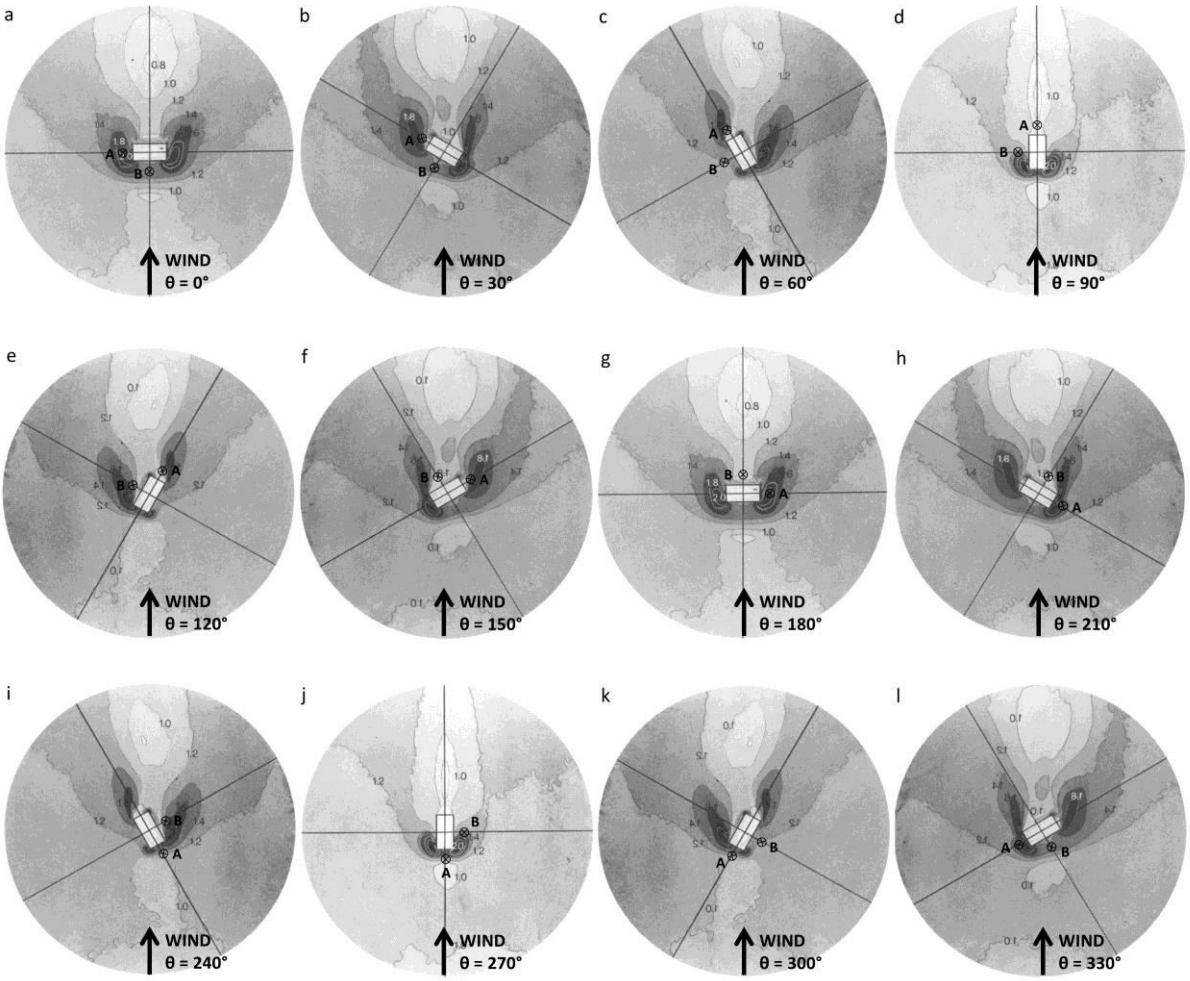

Figure 24. Sand erosion contours for a building with full-scale dimensions L x B x H = 40 x 20 x 70 m³. Indication of points A and B where wind comfort is evaluated (modified from [43]).

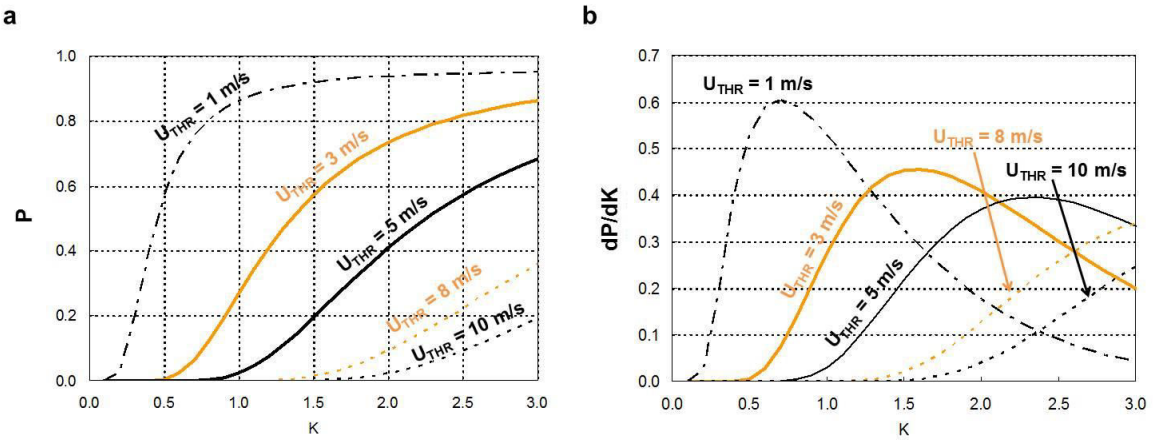

Figure 25. (a) Exceedance probability P as a function of local amplification factor K, with the threshold wind speed U_{THR} as parameter. (b) Sensitivity dP/dK as a function of K with U_{THR} as parameter.

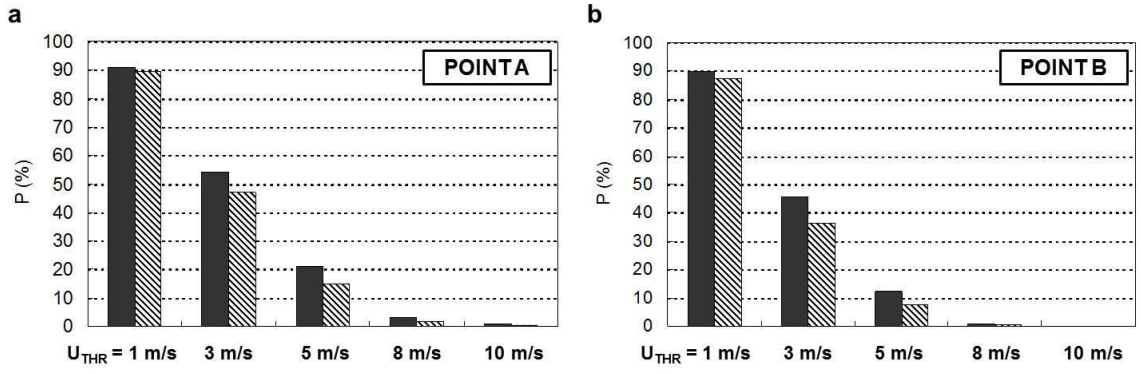

Figure 26. Exceedance probability P (%) in (a) point A and (b) point B, for different values of the threshold wind speed U_{THR}. The solid bars and the hashed bars represent results from the two sets of amplification factors.